Journal Pre-proof

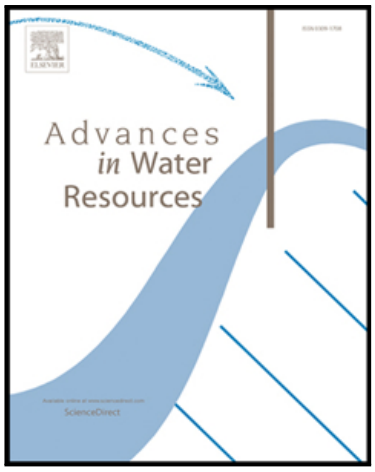


# The role of hydrology on enhanced weathering for carbon sequestration I. Modeling rock-dissolution reactions coupled to plant, soil moisture, and carbon dynamics

Giuseppe Cipolla, Salvatore Calabrese, Leonardo Valerio Noto, Amilcare Porporato

PII: S0309-1708(21)00089-0
DOI: https://doi.org/10.1016/j.advwatres.2021.103934
Reference: ADWR 103934

To appear in: *Advances in Water Resources*

Received date: 10 December 2020
Revised date: 23 March 2021
Accepted date: 24 April 2021

Please cite this article as: Giuseppe Cipolla, Salvatore Calabrese, Leonardo Valerio Noto, Amilcare Porporato, The role of hydrology on enhanced weathering for carbon sequestration I. Modeling rock-dissolution reactions coupled to plant, soil moisture, and carbon dynamics, *Advances in Water Resources* (2021), doi: https://doi.org/10.1016/j.advwatres.2021.103934

**The role of hydrology on enhanced weathering for carbon sequestration I. Modeling rock-dissolution reactions coupled to plant, soil moisture, and carbon dynamics:**

- A novel dynamic model connecting biogeochemical and ecohydrological dynamics to enhanced weathering is presented.
- Hydrological fluctuations lead to hysteretic patterns of weathering rates with soil moisture.
- Plants contribution to pH reduction and increased weathering rates during wet periods is quantified.

# The role of hydrology on enhanced weathering for carbon sequestration I. Modeling rock-dissolution reactions coupled to plant, soil moisture, and carbon dynamics

Giuseppe Cipolla[a], Salvatore Calabrese[b], Leonardo Valerio Noto[a], Amilcare Porporato[c]

[a]*Dipartimento di Ingegneria, Università degli Studi di Palermo, Palermo, Italy*
[b]*Department of Biological and Agricultural Engineering, Texas A&M University, College Station, TX, USA*
[c]*Department of Civil and Environmental Engineering, Princeton University, Princeton, NJ, USA*



**Abstract**

Enhanced Weathering (EW) resulting from soil amendment with highly reactive silicate minerals is regarded as one of the most effective techniques for carbon sequestration. While in laboratory conditions silicate minerals dissolution rates are well characterized, in field conditions the rate of the dissolution reaction is more difficult to predict, not least because it interacts with soil, plant, and hydrologic processes. Here we present a dynamic mass balance model connecting biogeochemical and ecohydrological dynamics to shed light on these intertwined processes involved in EW. We focus on the silicate mineral olivine, for its faster laboratory dissolution rate, and pay particular attention to understanding the role of plants and hydrological fluctuations and their propagation into soil biogeochemical processes (including cation exchange) and EW dynamics. A companion paper [1] presents specific applications with the main purpose of understanding the carbon sequestra-

tion potential under different climate scenarios.

*Keywords:* Enhanced Weathering, Carbon Sequestration, Climate Change

## 1. Introduction

To avoid climatic tipping points, the IPCC (Intergovernamental Panel on Climate Change) advocates for net-zero $CO_2$ emissions by 2030 [2, 3]. Achieving such goals might require a combination of low-emitting and CDR (Carbon Dioxide Removal) technologies [4], generally referred to as climate geoengineering. Among them, EW is considered as one of the most promising. However, a more in-depth knowledge of the interaction and feedbacks among the processes involving hydrology and soil biogeochemistry is necessary for large scales applications in natural environments.

Since $CO_2$ is the reactant of the weathering chemical reaction, EW is a negative emission technology [5, 6, 7] that sequesters atmospheric carbon and stores it in the oceans by leveraging key processes in soil formation, whereby primary minerals from the bedrock react with $CO_2$, dissolve, and generate secondary minerals. Because these reactions are mostly effective under hot and humid climates [8, 4], the presence of soil moisture is crucial to produce high mineral dissolution rates [9, 4]. Chemical Weathering is also favored by a high soil acidity, since $H^+$ ions are reactants in the weathering reactions [8, 4], and soil pH in turn is strongly dependent on soil moisture. The resulting processes thus form an interestingly intricate dynamical system defined by soil-plant conditions and forced by hydro-climatic conditions.

EW is achieved by adding highly reactive minerals, such as silicate minerals, to the soil [4]. Because of its high dissolution rate constant [10] and

relative abundance, forsterite or Mg-olivine ($Mg_2SiO_4$) is one of the best choices [6, 4]. In general, olivine may be a silicate of $Fe^{2+}$ (i.e. fayalite) or $Mg^{2+}$ (i.e. forsterite), but the latter is the most common choice [4, 7, 6] and is the one considered in this study (hereafter we will refer to it as olivine). Based on the reaction stoichiometry, the theoretical limit of sequestered $CO_2$ per given amount of olivine is equal to 1.25 $g_{CO_2}/g_{oliv}$ [6, 4]. To increase the exposed surface areas of particles and their dissolution rate, olivine is ground to diameters of a few hundred $\mu$m [7]. Averaging the costs of mining, grinding and transport operations, Köhler et al. [11] report a total cost of about 20 USD per ton of olivine, while the overall cost for sequestering $CO_2$ of about 20 USD per ton of sequestered $CO_2$. As an added cobenefit, olivine amendment leads to an increase of nutrients availability, especially $Mg^{2+}$ and $Ca^{2+}$, thus sustaining plant growth and in turn the weathering reaction itself [7].

Even if olivine dissolution dynamics in laboratory conditions is quite well known [12, 13], understanding and modeling the olivine dissolution in field conditions is still a challenge especially in relation to the observed reduced dissolution rates [14]. To help address this gap, Renforth et al. [7] and ten Berge et al. [6] conducted pot experiments to estimate the olivine weathering rate in soils extracted from agricultural fields. They found dissolution rates much lower (around $10^{-11}$mol $m^{-2}s^{-1}$) than those of laboratory experiments (around $10^{-8}$mol $m^{-2}s^{-1}$).

Given the urgency of the problem, models can play a very important role for extrapolating results of laboratory and field experiments in both time and space, as well as for quantifying the impact of hydroclimatic fluctuations on

the involved biogeochemical processes. In this paper we present a mathematical model coupling the key ecohydrological and biogeochemical aspects of EW to predict both carbon sequestration and increased nutrient availability in soil water. The model consists of interconnected components in terms of related differential equations describing the mass balance and the chemical reactions of the involved elements. Particular attention is paid to the soil moisture-soil pH dynamics, their connections to plant growth [15], as well as the relevance of the cation exchange process and plants uptake/release of ions on soil chemistry and weathering rate. The long-term role of hydrological processes on EW is captured by stochastic rainfall forcing which induces multiple combinations of wetting and drying phases which in time are responsible for the averaged weathering rates. The model can be forced with either actual precipitation measurements or with stochastic precipitation for long term simulations (e.g., Porporato et al. [16]).

The main motivation that inspired the development of this model was to understand the long-term role of hydrologic (i.e., soil moisture) variability, coupled to plant, organic matter and cation exchange dynamics on olivine weathering. In the past, reactive transport models have been used to simulate the interactions among plants and soil biogeochemistry, taking into account, in some cases, the EW process [5]. In most of the reactive transport models not all these processes are considered at the same time and the demanding numerical constraints of the vertically explicit formulation may limit the time horizon of their simulations. The model presented here is an attempt to go beyond these models by explicitly including the interactions between biotic and abiotic soil processes, while capturing long-term dynam-

ics and climate scenarios uncertainties with explicit inclusion of stochastic hydroclimatic forcing within an agile and relatively parsimonious modeling framework.

The paper is structured as follows. After an introduction to the structure of the model, section 2 presents the core of the model with a detailed description of all its components. In section 3 a reduced-order version of the model is presented. Section 4 provides the resolution of the model and some applications, highlighting the relevance of the wetting and drying phases on olivine weathering rate and the importance of modeling the cation exchange process and plants action on soil chemistry. Section 5 presents some discussions related to the novelty of this model compared to the existing reactive transport models and discusses some possible future improvements. Finally, in section 6 some conclusions concerning the model and its further applications are drawn. Cipolla et al. [1] describes specific applications of the model aimed at understanding the role of hydrological processes on olivine EW and provide useful information to guide the development of EW as a natural climate solution.

## 2. Modeling Scheme

The weathering process is strongly influenced by surface hydrological processes. Figure 1 highlights the main interactions with reference to the main model components, where the soil moisture dynamics resulting from the interaction between rainfall, soil and vegetation, influence soil biogeochemistry (i.e. the organic matter decomposition and the dissolved ions concentration in soil water), plants dynamics (i.e. uptake/release of ions which in turn

regulate pH levels in soil) and the olivine weathering rates.

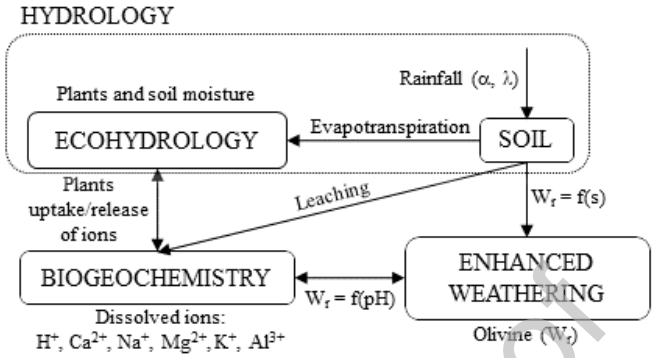


Figure 1: General scheme of the main model components and their interactions.

To account for long term hydrologic variability in present and future climates, a probabilistic rainfall description is used, where the rainfall characteristics, namely the average storm depth and frequency, are prescribed. For the sake of simplicity, the soil and vegetation parameters, such as the soil porosity, the typical water retention curve parameters, the cation exchange capacity parameters and the added litter from vegetation, are also given. A more detailed description of all the parameters of the model is provided in the companion paper which is specifically devoted to the applications [1]. Referring to a unit ground area of homogeneous soil comprising the root zone, the processes are resolved typically at a daily time scale.

A flow chart representative of the model structure is shown in figure 2. The central role of soil moisture on the whole system is clearly evident. Plants also play a relevant role on weathering, since the dissolved ions concentrations are regulated on the base of hydrological fluxes (i.e. leaching and evapotranspiration) and plants uptake/release of ions. The relevance of vegetation on EW and on soil chemistry is further highlighted in section 4.

The 'organic matter' component is related to the balance of soil organic carbon, which is one of the $CO_2$ sources in the system. The dissolved inorganic carbon (DIC) component includes the $CO_2$ in the gas phase and the part of it that reacts with water (i.e. green box within DIC). The 'Dissolved Minerals' component is related to all the dissolved elements which do not contain carbon, including the products of olivine dissolution (i.e. silicates and $Mg^{2+}$). The cation exchange capacity (CEC) describes the equilibrium exchanges between soil organic and inorganic colloids and the dissolved ions.

### *2.1. Olivine weathering reactions and balance*

The olivine weathering reaction can be written as follows,

$$Mg_2SiO_4 + 4\,CO_2 + 4\,H_2O \longrightarrow 2\,Mg^{2+} + 4\,HCO_3{}^- + H_4SiO_4, \tag{1}$$

or, to make the dependence on pH explicit, as [17],

$$Mg_2SiO_4 + 4\,H^+ \longrightarrow 2\,Mg^{2+} + H_2O + H_2SiO_3, \tag{2}$$

according to which one mole of olivine reacts with four moles of $H^+$ ions and results in two moles of $Mg^{2+}$ and one mole of silicic acid ($H_2SiO_3$).

The dissolution rate of olivine particles, expressed in number of moles of olivine per unit of reactive surface and per unit of time [14], is a function of soil moisture and pH [18, 19, 20],

$$W_r(s, pH) = s\,k_{sil}[H^+](1 - \frac{\Theta}{k_{eq}}), \tag{3}$$

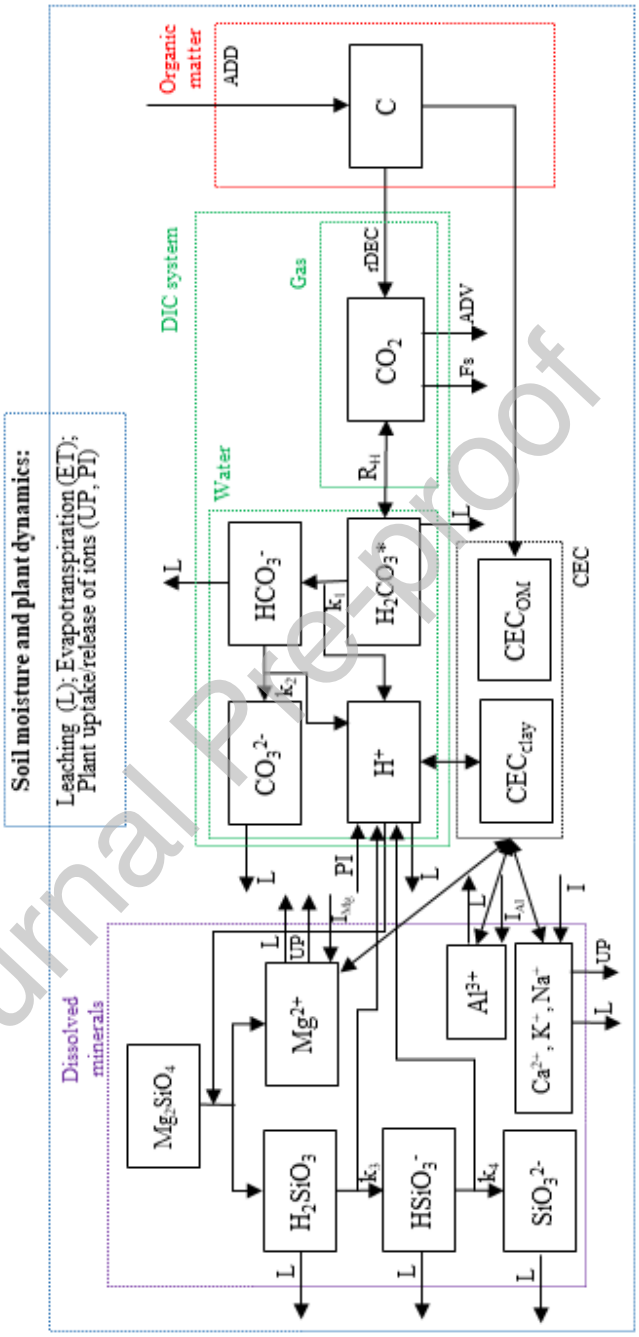


Figure 2: Flow chart of the involved fluxes in olivine weathering process.

where $k_{sil}$ is the dissolution rate constant of Forsterite [10]. To represent an average weathering rate at the Darcy scale considered here, such constant can be calibrated so as to obtain weathering rates of the same order of magnitude as those presented by Renforth et al. [7] and ten Berge et al. [6] (about $10^{-11}$mol m$^{-2}$s$^{-1}$), which are related to soil samples extracted from field. The linear dependence between weathering rate and soil moisture, $s$, is justified by the fact that soil moisture influences the fraction of surface areas of olivine particles exposed to weathering [9]. The dependence between weathering rate and pH is also defined by the ion activity product $\Theta$, which is the ratio between the product and reactant ions concentrations, elevated to their stoichiometric coefficients, in the chemical reaction (2). The equilibrium constant of reaction (2), $k_{eq}$, is from Morel and Hering [17],

$$\Theta = \frac{[Mg^{2+}]^{\frac{1}{2}}[\mathrm{H_2SiO_3}]^{\frac{1}{4}}}{[\mathrm{H^+}]}. \tag{4}$$

To account for the particle size distribution resulting from grinding operations, we consider an effective diameter, $\phi$, which can be defined as the mean diameter of a particle size distribution. This is consistent with the observation that the difference between the weathering rate integrated to the particle size distribution and the one calculated by only considering a single effective diameter is very low. This happens because particles with a diameter larger than the effective diameter are characterized by a higher reactive surface area, resulting in a higher pH increase at a certain time-step and in a lower weathering rate than the one related to the effective diameter (due to the higher pH). Since an opposite behavior characterizes those particles having a diameter lower than the effective diameter, weathering rates

of higher and lower particles diameters tend to compensate, justifying the adoption of an effective diameter. The reduction of the effective diameter can be modeled as the product between the weathering rate and the molar volume of olivine $V_M$ [10],

$$\frac{d\phi}{dt} = -W_r(s, pH)V_M. \tag{5}$$

*2.2. $CO_2$ source*

The $CO_2$ that reacts with olivine comes partly from the atmosphere (see Section 2.3) and partly from the respiration component of the soil organic matter decomposition. The latter is linked to mass balance of organic matter as [16, 21],

$$\frac{dC}{dt} = ADD - rDEC, \tag{6}$$

where (figure 2) $ADD$ is the added carbon (e.g., litterall, organic amendment) and $rDEC$ is the fraction of decomposed carbon that goes into respiration. The $ADD$ term can be either constant or a time-series. The term $DEC$ is assumed to linearly depend on the carbon concentration in soil, $C$, and on the carbon concentration of the microbial biomass, $C_b$, here assumed constant,

$$DEC = k_{dec} f_d(s) C C_b, \tag{7}$$

where $k_{dec}$ is a first order kinetic parameter representative of the carbon consumption and $f_d(s)$ is a nondimensional factor expressing the effects of soil moisture on carbon decomposition [16],

$$f_d(s) = \begin{cases} \frac{s}{s_{fc}} & s \leq s_{fc} \\ \frac{s_{fc}}{s} & s > s_{fc} \end{cases} \tag{8}$$

*2.3. $CO_2$ reactions and balance in water*

The $CO_2$ in the gas phase quickly reaches equilibrium with the dissolved $CO_2$ in the soil water, according to Henry's law (9). In general, the total concentration of dissolved $CO_2$, defined as $[H_2CO_3{}^*]$, can be expressed as the product of the Henry's constant ($K_H$) and the partial pressure of $CO_2$ ($P_{CO_2}$). The term $[H_2CO_3{}^*]$ was introduced since only a part of the dissolved $CO_2$ reacts with water and creates the carbonic acid ($H_2CO_3$), as it is expressed by equation (10),

$$[H_2CO_3{}^*] = K_H P_{CO_2}, \tag{9}$$

$$[H_2CO_3{}^*] = [H_2CO_3] + CO_{2,aq}. \tag{10}$$

The balance of gas plus dissolved $CO_2$ in the soil can be written as,

$$\frac{dCO_2}{dt} = rDEC - F_s - R_H - ADV. \tag{11}$$

The input of $CO_2$ in the DIC component is the output term of the organic matter component $rDEC$, described in Section 2.2. The term $F_s$ represents the amount of $CO_2$ released to the atmosphere due to soil respiration, $R_H$ is the mass flux of $CO_2$ due to the equilibrium of the gas-liquid phases, while $ADV$ is the advection flux of $CO_2$, meaning the $CO_2$ entering the soil during

the drying process and out of the soil during the wetting process. According to Daly et al. [22], $F_s$ can be estimated through the Fick's law, considering a one-dimensional flow,

$$F_s = D\frac{\mathrm{CO_2} - \mathrm{CO_{2,atm}}}{\frac{Z_r}{2}}, \tag{12}$$

where $D$ is the $CO_2$ diffusivity in the soil, while $CO_{2,atm}$ is the atmospheric $CO_2$ concentration and $Z_r/2$ is the average length of the diffusion path. $D$ can be evaluated as a function of the air-filled porosity, which summed to soil moisture equals 1, and the total porosity, $n$, [23],

$$D = D_0\frac{(1-s)^{10/3}}{n^2}, \tag{13}$$

where the term $D_0$ is the free-air diffusion coefficient of $CO_2$. The term $ADV$ can be estimated through the following equations,

$$ADV = \begin{cases} nZr\frac{ds}{dt}\mathrm{CO_{2,atm}} & \frac{ds}{dt} < 0 \\ nZr\frac{ds}{dt}\mathrm{CO_{2,air}} & \frac{ds}{dt} > 0 \end{cases} \tag{14}$$

During soil drying, air with $CO_{2,atm}$ enters the soil pores; during wetting, part of the soil air at $CO_{2,air}$ concentration is pumped out the system.

### *2.4. Differential balance equations of ions in water*

#### *2.4.1. Carbonate ions and pH balance equations*

The DIC component regulates the time evolution of soil pH and in turn the weathering reaction. The carbonic acid produced by the $CO_2$ dissolution rapidly dissociates in its deprotonated forms,

$$H_2CO_3{}^* \overset{k_1}{\rightleftharpoons} H^+ + HCO_3{}^-, \tag{15}$$

$$HCO_3{}^- \overset{k_2}{\rightleftharpoons} H^+ + CO_3{}^{2-}. \tag{16}$$

These two reactions are strictly connected to the weathering reaction (2) since they provide the $H^+$ ions that react with olivine. Another source of $H^+$ ions is the self-ionization of water,

$$H_2O \overset{k_w}{\rightleftharpoons} H^+ + OH^-. \tag{17}$$

Based on the chemical reactions (15), (16) and (17), the mass balance equations for the *DIC* system can be written as,

$$nZr\frac{ds[H_2CO_3{}^*]}{dt} = -L_{H_2CO_3{}^*} - R_1 + R_H, \tag{18}$$

$$nZr\frac{ds[HCO_3{}^-]}{dt} = -L_{HCO_3{}^-} + R_1 - R_2, \tag{19}$$

$$nZr\frac{ds[CO_3{}^{2-}]}{dt} = -L_{CO_3{}^{2-}} + R_2, \tag{20}$$

$$nZr\frac{ds[H^+]}{dt} = PI + RI - L_{H^+} + R_1 + R_2 + R_3 + R_w + 3R_{Al^{3+}} + \tag{21}$$
$$- W_{bg} - 4W_{oliv} - \frac{dx_{H^+_{OM}}}{dt} - \frac{dx_{H^+_{clay}}}{dt},$$

$$nZr\frac{ds[OH^-]}{dt} = -L_{OH^-} + R_w. \tag{22}$$

Equation (21) is very important for the model since it is representative of pH time dynamics. The *PI* (Plant Input) term stands for the input concentration of $H^+$ ions from vegetation, while the *RI* (Rainfall Input) term

represents the input of $H^+$ connected to the infiltration rate. The term $W_{bg}$ is the background weathering, illustrative of the $H^+$ losses due to naturally present soil minerals, excluding olivine, while the $H^+$ losses due to olivine weathering are represented by the term $W_{oliv}$. The two time derivatives of $x_{H^+_{OM}}$ and $x_{H^+_{clay}}$ are related to the cation exchanges of dissolved $H^+$ with soil organic and clay colloids. The terms $R_j$ of equations (18-22) are the mass fluxes of the dissolved minerals due to the related chemical reactions (the subscripts of the terms $R_j$ are the same of those of the equilibrium constants in the corresponding reactions). DIC ions are all affected by leaching, generally written as,

$$L_{\mathrm{X}} = \frac{L(s)}{snZ_r}[\mathrm{X}], \tag{23}$$

where [X] indicates the concentration of the dissolved ion of interest.

The passive uptake of macro-nutrients, such as magnesium, calcium, and potassium, and of the micro-nutrient sodium is here modeled as proportional to the transpiration rate, $T(s)$, [16],

$$UP_{\mathrm{X}} = \frac{T(s)}{snZ_r}[\mathrm{X}]. \tag{24}$$

Since plants tend to maintain a neutral charge [8], if they take up from the soil water more cations than anions, they release $H^+$ ions to balance the charges. The release of plant $H^+$ can thus be calculated based on the uptake of cations and their corresponding valence as,

$$PI = 2UP_{\mathrm{Mg^{2+}}} + 2UP_{\mathrm{Ca^{2+}}} + UP_{\mathrm{K^{+}}} + UP_{\mathrm{Na^{+}}}. \tag{25}$$

Typically, rain is characterized by a slightly acidic pH (about 5.6) because of the presence of carbonic acid due to the chemical reaction between $CO_2$ and water in the atmosphere [24]. Therefore, the term $RI$ can be written as proportional to the dimensionless infiltration rate, $I(s)$, defined by the soil water balance (see section 2.5), and to the $H^+$ concentration at a pH level of 5.6,

$$RI = \frac{I(s)}{snZ_r} 10^{-5.6}. \tag{26}$$

The weathering of all naturally present soil minerals is accounted for in equation (21) by the background weathering, $W_{bg}$. The latter groups in a single sink term the consumption of $H^+$ by the dissolution of various minerals,

$$W_{bg} = s\, k_{bg}[H^+] A(d_{bg}) \frac{f_{bg}\rho_b(1-n)Z_r}{\rho_{bg}V_{bg}}, \tag{27}$$

which is proportional to the reactive surface areas of the mineral particles (the product between soil moisture, $s$, and the geometric surface area of particles, $A(d_{bg})$), the effective dissolution rate constant, $k_{bg}$, the $H^+$ concentration, and the mass of the minerals in the soil, which can be estimated, for the sake of simplicity, as a percentage of the total mass of the soil. The effective dissolution rate constant and the geometric surface area should take into account the composition of the soil, in particular the minerals contributing more to the consumption of $H^+$. For example, pedogenic carbonate minerals (i.e., $MgCO_3$ and $CaCO_3$) can be the dominant $H^+$ sink in very dry soils, due to the low leaching of ${CO_3}^{2-}$. In this case, the effective dissolution rate

constant should reflect more the dissolution of carbonates, rather than silicates. In general, $W_{bg}$ is a flexible term that should be calibrated based on the estimated composition of the soil under study.

The term $W_{oliv}$, representative of the $H^+$ loss due to olivine dissolution, can be written as,

$$W_{oliv} = A(\phi) W_r \frac{M_{oliv}}{\rho_{oliv} V_{oliv}}. \tag{28}$$

By writing $W_r$ as in equation (3), the product between soil moisture and the geometric surface area of olivine particles is recognized as the reactive surface area, as explained by Sverdrup and Warfvinge [9]. In eq. (21), $W_{oliv}$ is multiplied by a coefficient equal to 4, since one mole of olivine reacts with four moles of $H^+$, as highlighted in the reaction (2).

The last two terms of equation (21) are related to the cation exchanges between soil colloids and solution. The CEC is a measure of the amount of moles of cations that can be adsorbed on soil colloids (due to their negatively charged surface [25]) and can be described by the following equilibrium reactions, where X and M are two generic cations that are dissolved and adsorbed, respectively. The terms $x$ and $m$ are the respective charges of the two cations.

$$\frac{1}{\mathrm{x}}\mathrm{X}^{x+} + \frac{1}{\mathrm{m}}\mathrm{M}^{m+} CEC_{OM} \underset{}{\overset{SC_{OM}(\mathrm{X}-\mathrm{M})}{\rightleftharpoons}} \frac{1}{\mathrm{x}}\mathrm{X}^{x+} CEC_{OM} + \frac{1}{\mathrm{m}}\mathrm{M}^{m+} \tag{29}$$

$$\frac{1}{\mathrm{x}}\mathrm{X}^{x+} + \frac{1}{\mathrm{m}}\mathrm{M}^{m+} CEC_{clay} \underset{}{\overset{SC_{clay}(\mathrm{X}-\mathrm{M})}{\rightleftharpoons}} \frac{1}{\mathrm{x}}\mathrm{X}^{x+} CEC_{clay} + \frac{1}{\mathrm{m}}\mathrm{M}^{m+} \tag{30}$$

The total CEC of the soil includes the organic matter ($CEC_{OM}$) and the clay components ($CEC_{clay}$), which represent, respectively, the exchanges

occurring in organic and inorganic sites of the soil, better known as organic and clay colloids. The first is evaluated as the product between the typical specific CEC of organic colloids [8] and the total mass of organic carbon in the soil, obtained through equation (6). Similarly, the $CEC_{clay}$ is the product between the typical specific CEC of clay colloids and the total mass of clay in the soil, fixed as a percentage of the total mass of the soil. Here, we consider explicitly the exchange of $H^+$, $Na^+$, $Ca^{2+}$, $K^+$, $Al^{3+}$ and $Mg^{2+}$, because of their widespread presence in soils and because $K^+$, $Ca^{2+}$ and $Mg^{2+}$ are the most common macro-nutrients for plants. Depending on the exchange processes and particularly on the amount of $H^+$ adsorbed on soil colloids, there is a change in soil pH which influences the olivine weathering reaction. We compute the amount of adsorbed ions in the soil sites based on the Gapon equation [26], which considers equilibrium reactions between dissolved and adsorbed ions and assumes a fixed number of exchanges adsorption sites [27]. With reference to the binary exchange between $H^+$ and $Ca^{2+}$, one can write the mass of exchanged hydrogen ions in the organic and clay colloids as,

$$x_{\mathrm{H^+_{OM}}} = \frac{CEC_{OM} - x_{\mathrm{Na^+_{OM}}} - x_{\mathrm{Mg^{2+}_{OM}}} - x_{\mathrm{K^+_{OM}}} - x_{\mathrm{Al^{3+}_{OM}}}}{[1 + \frac{1}{SC_{OM}(\mathrm{H^+ - Ca^{2+}})\frac{[\mathrm{H^+}]}{[\mathrm{Ca^{2+}}]^{\frac{1}{2}}}}]}, \tag{31}$$

$$x_{\mathrm{H^+_{clay}}} = \frac{CEC_{clay} - x_{\mathrm{Na^+_{clay}}} - x_{\mathrm{Mg^{2+}_{clay}}} - x_{\mathrm{K^+_{clay}}} - x_{\mathrm{Al^{3+}_{clay}}}}{[1 + \frac{1}{SC_{clay}(\mathrm{H^+ - Ca^{2+}})\frac{[\mathrm{H^+}]}{[\mathrm{Ca^{2+}}]^{\frac{1}{2}}}}]}. \tag{32}$$

In equations (31, 32), the exchanged $Na^+$, $K^+$, $Al^{3+}$ and $Mg^{2+}$ are subtracted to the $CEC_{OM}$ and $CEC_{clay}$ since the portions of colloids occupied by these cations cannot be used for the exchange between $H^+$ and $Ca^{2+}$. This aspect highlights the competition among all the dissolved ions, in this

case $H^+$, $Ca^{2+}$, $Mg^{2+}$, $K^+$, $Al^{3+}$ and $Na^+$, in the neutralization of the negative charges of soil colloids. The terms $SC_{OM}(H^+ - Ca^{2+})$ and $SC_{clay}(H^+ - Ca^{2+})$ are the binary selectivity constants between $H^+$ and $Ca^{2+}$, while in square brackets there are the concentrations of dissolved $H^+$ and $Ca^{2+}$.

*2.4.2. Aluminum hydrolysis and exchange*

Aluminum hydrolysis represents one of the major $H^+$ sources in acid soils [8]. The dissolution of parent materials, such as gibbsite, releases $Al^{3+}$ ions in soil water that react as,

$$\begin{cases} Al^{3+} + H_2O <=> Al(OH)^{2+} + H^+ \\ Al(OH)^{2+} + H_2O <=> Al(OH)_2{}^+ + H^+ \\ Al(OH)_2{}^+ + H_2O <=> Al(OH)_3 + H^+ \end{cases} \tag{33}$$

If combined, these reactions result in

$$Al^{3+} + 3\,H_2O \underset{}{\overset{R_{Al^{3+}}}{\rightleftharpoons}} Al(OH)_3 + 3\,H^+. \tag{34}$$

The balance of $Al^{3+}$ can thus be expressed as,

$$nZr\frac{ds[Al^{3+}]}{dt} = I_{Al^{3+}} - L_{Al^{3+}} - R_{Al^{3+}} - \frac{dx_{Al^{3+}_{OM}}}{dt} - \frac{dx_{Al^{3+}_{clay}}}{dt}, \tag{35}$$

where $I_{Al^{3+}}$ represents the input concentration of $Al^{3+}$ in the system. This is related to the dissolution of parent materials and can be expressed through an expression similar to (27), i.e., as a function of the dissolution rate of the parent material. The output of $Al^{3+}$ is related to leaching, $L_{Al^{3+}}$, while $R_{Al^{3+}}$

is the mass flux due to the hydrolysis reaction (34). The last two terms of equation (35) are related to the cation exchanges with organic matter and clay colloids. The moles of exchanged $Al^{3+}$ per unit mass of reactive soil are:

$$x_{\mathrm{Al^{3+}_{OM}}} = \frac{CEC_{OM} - x_{\mathrm{H^{+}_{OM}}} - x_{\mathrm{Mg^{2+}_{OM}}} - x_{\mathrm{Ca^{2+}_{OM}}} - x_{\mathrm{K^{+}_{OM}}}}{[1 + \frac{1}{SC_{OM}(\mathrm{Al^{3+}} - \mathrm{Na^{+}})\frac{[\mathrm{Al^{3+}}]^{\frac{1}{3}}}{[\mathrm{Na^{+}}]}}]}, \tag{36}$$

$$x_{\mathrm{Al^{3+}_{clay}}} = \frac{CEC_{clay} - x_{\mathrm{H^{+}_{clay}}} - x_{\mathrm{Mg^{2+}_{clay}}} - x_{\mathrm{Ca^{2+}_{clay}}} - x_{\mathrm{K^{+}_{clay}}}}{[1 + \frac{1}{SC_{clay}(\mathrm{Al^{3+}} - \mathrm{Na^{+}})\frac{[\mathrm{Al^{3+}}]^{\frac{1}{3}}}{[\mathrm{Na^{+}}]}}]}. \tag{37}$$

*2.4.3. Nutrients balance equations*

The mass balance equations of $Mg^{2+}$, $Ca^{2+}$, $K^{+}$ and $Na^{+}$ can be written as,

$$nZr\frac{ds[\mathrm{Mg^{2+}}]}{dt} = I_{\mathrm{Mg^{2+}}} - L_{\mathrm{Mg^{2+}}} - UP_{\mathrm{Mg^{2+}}} + 2W_{oliv} - \frac{dx_{\mathrm{Mg^{2+}_{OM}}}}{dt} - \frac{dx_{\mathrm{Mg^{2+}_{clay}}}}{dt}, \tag{38}$$

$$nZr\frac{ds[\mathrm{Ca^{2+}}]}{dt} = I_{\mathrm{Ca^{2+}}} - L_{\mathrm{Ca^{2+}}} - UP_{\mathrm{Ca^{2+}}} - \frac{dx_{\mathrm{Ca^{2+}_{OM}}}}{dt} - \frac{dx_{\mathrm{Ca^{2+}_{clay}}}}{dt}, \tag{39}$$

$$nZr\frac{ds[\mathrm{K^{+}}]}{dt} = I_{\mathrm{K^{+}}} - L_{\mathrm{K^{+}}} - UP_{\mathrm{K^{+}}} - \frac{dx_{\mathrm{K^{+}_{OM}}}}{dt} - \frac{dx_{\mathrm{K^{+}_{clay}}}}{dt}, \tag{40}$$

$$nZr\frac{ds[\mathrm{Na^{+}}]}{dt} = I_{\mathrm{Na^{+}}} - L_{\mathrm{Na^{+}}} - UP_{\mathrm{Na^{+}}} - \frac{dx_{\mathrm{Na^{+}_{OM}}}}{dt} - \frac{dx_{\mathrm{Na^{+}_{clay}}}}{dt}. \tag{41}$$

For each of these cations, the input term, $I$, includes the atmospheric deposition, the return of cations from plant litter and an input from the dissolution of minerals within the soil. These three terms vary according to different time scales. For instance, the return of cations from vegetation should be linked to the decomposition of the soil litter (i.e., the term DEC), while the input from minerals should be defined based on the corresponding dissolution rates. However, because these inputs are small and we are interested in the long-term (i.e., the scale of the olivine weathering process), they may be grouped in a single constant. Furthermore, $Mg^{2+}$ has an additional input due to the weathering of olivine, i.e., one mole of olivine releases two moles of $Mg^{2+}$ according to reaction (2). For all the ions, losses are represented by leaching, plant uptake and cation exchange terms. The moles of exchanged $Mg^{2+}$, $K^+$ and $Na^+$ per unit of mass of reactive soil are related by,

$$x_{\mathrm{Mg^{2+}_{OM}}} = \frac{CEC_{OM} - x_{\mathrm{Na^{+}_{OM}}} - x_{\mathrm{H^{+}_{OM}}} - x_{\mathrm{K^{+}_{OM}}} - x_{\mathrm{Al^{3+}_{OM}}}}{[1 + \frac{1}{SC_{OM}(\mathrm{Ca^{2+}} - \mathrm{Mg^{2+}})\frac{[\mathrm{Mg^{2+}}]}{[\mathrm{Ca^{2+}}]}}]}, \tag{42}$$

$$x_{\mathrm{Mg^{2+}_{clay}}} = \frac{CEC_{clay} - x_{\mathrm{Na^{+}_{clay}}} - x_{\mathrm{H^{+}_{clay}}} - x_{\mathrm{K^{+}_{clay}}} - x_{\mathrm{Al^{3+}_{clay}}}}{[1 + \frac{1}{SC_{clay}(\mathrm{Ca^{2+}} - \mathrm{Mg^{2+}})\frac{[\mathrm{Mg^{2+}}]}{[\mathrm{Ca^{2+}}]}}]}, \tag{43}$$

$$x_{\mathrm{K^{+}_{OM}}} = \frac{CEC_{OM} - x_{\mathrm{H^{+}_{OM}}} - x_{\mathrm{Mg^{2+}_{OM}}} - x_{\mathrm{Ca^{2+}_{OM}}} - x_{\mathrm{Al^{3+}_{OM}}}}{[1 + \frac{1}{SC_{OM}(\mathrm{K^{+}} - \mathrm{Na^{+}})\frac{[\mathrm{K^{+}}]}{[\mathrm{Na^{+}}]}}]}, \tag{44}$$

$$x_{\mathrm{K^{+}_{clay}}} = \frac{CEC_{clay} - x_{\mathrm{H^{+}_{clay}}} - x_{\mathrm{Mg^{2+}_{clay}}} - x_{\mathrm{Ca^{2+}_{clay}}} - x_{\mathrm{Al^{3+}_{clay}}}}{[1 + \frac{1}{SC_{clay}(\mathrm{K^{+}} - \mathrm{Na^{+}})\frac{[\mathrm{K^{+}}]}{[\mathrm{Na^{+}}]}}]}, \tag{45}$$

$$x_{\mathrm{Na^+_{OM}}} = \frac{CEC_{OM} - x_{\mathrm{H^+_{OM}}} - x_{\mathrm{Mg^{2+}_{OM}}} - x_{\mathrm{K^+_{OM}}} - x_{\mathrm{Al^{3+}_{OM}}}}{[1 + \frac{1}{SC_{OM}(\mathrm{Na^+ - Ca^{2+}})\frac{[\mathrm{Na^+}]}{[\mathrm{Ca^{2+}}]^{\frac{1}{2}}}}]}, \tag{46}$$

$$x_{\mathrm{Na^+_{clay}}} = \frac{CEC_{clay} - x_{\mathrm{H^+_{clay}}} - x_{\mathrm{Mg^{2+}_{clay}}} - x_{\mathrm{K^+_{clay}}} - x_{\mathrm{Al^{3+}_{clay}}}}{[1 + \frac{1}{SC_{clay}(\mathrm{Na^+ - Ca^{2+}})\frac{[\mathrm{Na^+}]}{[\mathrm{Ca^{2+}}]^{\frac{1}{2}}}}]}, \tag{47}$$

$$CEC_{OM} = x_{\mathrm{H^+_{OM}}} + x_{\mathrm{Na^+_{OM}}} + x_{\mathrm{Ca^{2+}_{OM}}} + x_{\mathrm{Mg^{2+}_{OM}}} + x_{\mathrm{K^+_{OM}}} + x_{\mathrm{Al^{3+}_{OM}}}, \tag{48}$$

$$CEC_{clay} = x_{\mathrm{H^+_{clay}}} + x_{\mathrm{Na^+_{clay}}} + x_{\mathrm{Ca^{2+}_{clay}}} + x_{\mathrm{Mg^{2+}_{clay}}} + x_{\mathrm{K^+_{clay}}} + x_{\mathrm{Al^{3+}_{clay}}}. \tag{49}$$

Equations (48) and (49) define the total CEC of organic and clay colloids as the sum between the total amount of exchanged ions taken into account in our system.

*2.4.4. Silicates balance equations*

The silicic acid dissociation depends on pH. More specifically, if pH is less than 8, silicic acid remains in the form of the undissociated $H_2SiO_3$. If pH is within the range 8-13, silicic acid deprotonates in the form of $HSiO_3{}^-$, while if the pH is higher than 13, the second dissociation occurs and silicic acid will also be in the form of $SiO_3{}^{2-}$.

$$\begin{cases} \mathrm{H_2SiO_3} & pH < 8 \\ \mathrm{H_2SiO_3} \overset{k_3}{\rightleftharpoons} \mathrm{HSiO_3{}^- + H^+} & 8 \leq pH < 13 \\ \mathrm{HSiO_3{}^-} \overset{k_4}{\rightleftharpoons} \mathrm{SiO_3{}^{2-} + H^+} & pH \geq 13 \end{cases} \tag{50}$$

The balance of silicates can be written as,

$$nZr\frac{ds[\mathrm{H_2SiO_3}]}{dt} = -L_{\mathrm{H_2SiO_3}} + W_{oliv} - R_3, \tag{51}$$

$$nZr\frac{ds[\mathrm{HSiO_3}^-]}{dt} = -L_{\mathrm{HSiO_3}^-} + R_3 - R_4, \tag{52}$$

$$nZr\frac{ds[\mathrm{SiO_3}^{2-}]}{dt} = -L_{\mathrm{SiO_3}^{2-}} + R_4. \tag{53}$$

Apart from reaction rates and leaching losses, equation (51) presents a gain of $H_2SiO_3$ due to the weathering of olivine. It reflects the fact that for one mole of olivine that reacts, one mole of $H_2SiO_3$ is produced, according to the weathering reaction (2).

*2.5. Soil moisture dynamics*

Soil moisture dynamics for a root zone depth $Z_r$ is [16]

$$nZ_r\frac{ds}{dt} = I(s,t) - E(s) - T(s) - L(s). \tag{54}$$

The infiltration rate from rainfall, $I(s,t)$, is a function of soil moisture and time and is evaluated as the minimum value among the rainfall depth and the amount of water that can be stored in the soil at a certain soil moisture value. Rainfall can be obtained from time-series or modeled as a marked Poisson process, in which the frequency of rainfall events is represented by the parameter $\lambda$ and the mean rainfall depth by the parameter $\alpha$ [28]. Bare soil evaporation is $E(s)$ and the transpiration rate, $T(s)$, are evaluated as in Porporato et al. [16]. The term $L(s)$ is representative of the leakage losses, evaluated as a function of soil moisture, through an exponential law, which

includes the hydraulic conductivity at saturation, $K_s$, the soil moisture at the field capacity, $s_{fc}$, and the pore size distribution index.

## 3. Reduced-order model

The equations representative of the biogeochemical, ecohydrological, and EW processes constitute a complex system of equations, which are partly differential and partly algebraic. Several of these equations can be combined to obtain a reduced-order version of the model. In particular, analyzing equations (55) and (56) one can notice that an equation for the total carbon $C_t$ is obtained by combining equations (11), (18), (19) and (20),

$$C_{DIC} = [\mathrm{H_2CO_3}^*] + [\mathrm{HCO_3}^-] + [\mathrm{CO_3}^{2-}], \tag{55}$$

$$C_t = [\mathrm{CO_{2,air}}] + C_{DIC}, \tag{56}$$

$$\frac{dC_t}{dt} = rDEC - F_s - ADV - L_{C_{DIC}}, \tag{57}$$

which allows us to simplify the equilibrium terms, $R_j$, and reduce four equations into only one.

The equilibrium constants of the dissolved inorganic carbon reactions can be written as [4],

$$K_{H,ad} = \frac{[\mathrm{H_2CO_3}^*]}{[\mathrm{CO_{2,air}}]}, \tag{58}$$

$$k_1 = \frac{[\mathrm{HCO_3}^-][\mathrm{H}^+]}{[\mathrm{H_2CO_3}^*]}, \tag{59}$$

$$k_2 = \frac{[\mathrm{CO_3}^{2-}][\mathrm{H}^+]}{[\mathrm{HCO_3}^-]}. \tag{60}$$

In equation (58) the ratio between the concentration of carbonic acid and the $CO_2$ concentration in the gas phase is the dimensionless Henry's constant, equal to 0.83. The equilibrium constants of the first and the second order of carbonic acid dissociation are indicated with $k_1$ and $k_2$, respectively. By combining the expressions (58-60), it is possible to write each element of the dissolved inorganic carbon as a fraction of $C_{DIC}$ [29],

$$[H_2CO_3{}^*] = \alpha_0 C_{DIC}, \tag{61}$$

$$[HCO_3{}^-] = \alpha_1 C_{DIC}, \tag{62}$$

$$[CO_3^{2-}] = \alpha_2 C_{DIC}, \tag{63}$$

where the coefficients $\alpha_0$, $\alpha_1$ and $\alpha_2$ depend on pH, as shown by the following equations,

$$\alpha_0 = (1 + \frac{k_1}{[H^+]} + \frac{k_1 k_2}{[H^+]^2})^{-1}, \tag{64}$$

$$\alpha_1 = (\frac{[H^+]}{k_1} + 1 + \frac{k_2}{[H^+]})^{-1}, \tag{65}$$

$$\alpha_2 = (\frac{[H^+]^2}{k_1 k_2} + \frac{[H^+]}{k_2} + 1)^{-1}. \tag{66}$$

Another important parameter is the alkalinity,

$$A = [HCO_3{}^-] + 2[CO_3^{2-}] - [H^+] - 3[Al^{3+}] + [OH^-], \tag{67}$$

that considering equations (61-63) can be written as

$$A = C_{DIC}(\alpha_1 + 2\alpha_2) - [\mathrm{H}^+] - 3[\mathrm{Al}^{3+}] + [\mathrm{OH}^-]. \tag{68}$$

Since in the mass balance differential equations related to $\mathrm{H}^+$ (eq. 21) and $\mathrm{Al}^{3+}$ (eq. 35) there are also the cation exchange capacity terms, the alkalinity expression can be modified by introducing the total $\mathrm{H}^+$ and $\mathrm{Al}^{3+}$ instead of the dissolved $\mathrm{H}^+$ and $\mathrm{Al}^{3+}$, defined as the sum between the dissolved and adsorbed moles of $\mathrm{H}^+$ and $\mathrm{Al}^{3+}$ in soil colloids,

$$\mathrm{H}_\mathrm{t}^+ = \mathrm{H}^+ + x_{\mathrm{H}_{\mathrm{OM}}^+} + x_{\mathrm{H}_{\mathrm{clay}}^+}, \tag{69}$$

$$\mathrm{Al}_t^{3+} = \mathrm{Al}^{3+} + x_{\mathrm{Al}_{OM}^{3+}} + x_{\mathrm{Al}_{clay}^{3+}}. \tag{70}$$

The expression for the total alkalinity is thus,

$$A_t = C_{DIC}(\alpha_1 + 2\alpha_2) - [\mathrm{H}_\mathrm{t}^+] - 3[\mathrm{Al}_t^{3+}] + [\mathrm{OH}^-], \tag{71}$$

whose balance equation reads

$$\frac{dA_t}{dt} = -L_{\mathrm{HCO_3^-}} - 2L_{\mathrm{CO_3^{2-}}} - RI - PI + L_{\mathrm{H^+}} - L_{\mathrm{OH^-}} + \tag{72}$$
$$+ W_{bg} + 4W_{oliv} - 3I_{\mathrm{Al^{3+}}} + 3L_{\mathrm{Al^{3+}}}.$$

Similarly, we introduce the total masses of calcium, magnesium, potassium, sodium and aluminum and the corresponding mass balance differential equations,

$$\mathrm{Ca_t^{2+}} = \mathrm{Ca^{2+}} + x_{\mathrm{Ca^{2+}_{OM}}} + x_{\mathrm{Ca^{2+}_{clay}}}, \tag{73}$$

$$\mathrm{Mg_t^{2+}} = \mathrm{Mg^{2+}} + x_{\mathrm{Mg^{2+}_{OM}}} + x_{\mathrm{Mg^{2+}_{clay}}}, \tag{74}$$

$$\mathrm{K_t^{+}} = \mathrm{K^{+}} + x_{\mathrm{K^{+}_{OM}}} + x_{\mathrm{K^{+}_{clay}}}, \tag{75}$$

$$\mathrm{Na_t^{+}} = \mathrm{Na^{+}} + x_{\mathrm{Na^{+}_{OM}}} + x_{\mathrm{Na^{+}_{clay}}}, \tag{76}$$

$$\frac{d\mathrm{Ca_t^{2+}}}{dt} = I_{\mathrm{Ca^{2+}}} - L_{\mathrm{Ca^{2+}}} - UP_{\mathrm{Ca^{2+}}}, \tag{77}$$

$$\frac{d\mathrm{Mg_t^{2+}}}{dt} = I_{\mathrm{Mg^{2+}}} - L_{\mathrm{Mg^{2+}}} - UP_{\mathrm{Mg^{2+}}} + 2W_{oliv}, \tag{78}$$

$$\frac{d\mathrm{K_t^{+}}}{dt} = I_{\mathrm{K^{+}}} - L_{\mathrm{K^{+}}} - UP_{\mathrm{K^{+}}}, \tag{79}$$

$$\frac{d\mathrm{Na_t^{+}}}{dt} = I_{\mathrm{Na^{+}}} - L_{\mathrm{Na^{+}}} - UP_{\mathrm{Na^{+}}}, \tag{80}$$

$$\frac{d\mathrm{Al_t^{3+}}}{dt} = I_{\mathrm{Al^{3+}}} - L_{\mathrm{Al^{3+}}}. \tag{81}$$

The equations for the silicates (51-53) can be condensed into one equation, defining the total silicon in the system as the sum of all the three forms of this element,

$$\mathrm{Si_t} = \mathrm{H_2SiO_3} + \mathrm{HSiO_3^{-}} + \mathrm{SiO_3^{2-}}, \tag{82}$$

$$\frac{d\mathrm{Si_t}}{dt} = -L_{\mathrm{Si_t}} + W_{oliv}. \tag{83}$$

## 4. Model Summary and Numerical Simulations

At this point, before delving into the simulations, it is useful to take stock and present here a synopsis of the model. The time dynamics of the total carbon, the total alkalinity and the mass of the total calcium, sodium,

magnesium, potassium, aluminum and silicates are described by the following mass balance differential equations.

$$\begin{cases} \frac{dC_t}{dt} = rDEC - F_s - ADV - L_{C_{DIC}} \\ \frac{dA_t}{dt} = -L_{\mathrm{HCO_3^-}} - 2L_{\mathrm{CO_3^{2-}}} - RI - PI + L_{\mathrm{H^+}} + \\ -L_{\mathrm{OH^-}} + W_{bg} + 4W_{oliv} - 3I_{\mathrm{Al^{3+}}} + 3L_{\mathrm{Al^{3+}}} \\ \frac{d\mathrm{Ca_t^{2+}}}{dt} = I_{\mathrm{Ca^{2+}}} - L_{\mathrm{Ca^{2+}}} - UP_{\mathrm{Ca^{2+}}} \\ \frac{d\mathrm{Mg_t^{2+}}}{dt} = I_{\mathrm{Mg^{2+}}} - L_{\mathrm{Mg^{2+}}} - UP_{\mathrm{Mg^{2+}}} + 2W_{oliv} \\ \frac{d\mathrm{Na_t^{+}}}{dt} = I_{\mathrm{Na^{+}}} - L_{\mathrm{Na^{+}}} - UP_{\mathrm{Na^{+}}} \\ \frac{d\mathrm{K_t^{+}}}{dt} = I_{\mathrm{K^{+}}} - L_{\mathrm{K^{+}}} - UP_{\mathrm{K^{+}}} \\ \frac{d\mathrm{Al_t^{3+}}}{dt} = I_{\mathrm{Al^{3+}}} - L_{\mathrm{Al^{3+}}} \\ \frac{d\mathrm{Si_t}}{dt} = -L_{\mathrm{Si_t}} + W_{oliv} \end{cases} \tag{84}$$

The system of equations (84) is here solved in an explicit way with a forward scheme, once the initial conditions for $C_t$, $A_t$, $\mathrm{Ca_t^{2+}}$, $\mathrm{Mg_t^{2+}}$, $\mathrm{Na_t^{+}}$,$\mathrm{K_t^{+}}$, $\mathrm{Al_t^{3+}}$ and $\mathrm{Si_t}$ are fixed. The concentration of the considered dissolved ions ($\mathrm{Ca^{2+}}$, $\mathrm{Na^{+}}$, $\mathrm{Mg^{2+}}$, $\mathrm{H^{+}}$, $\mathrm{K^{+}}$, $\mathrm{Al^{3+}}$) and other individual variables are obtained by solving an implicit algebraic system (see Appendix A for the derivation).

The initial condition of the total carbon, $C_t$, has been defined as the sum of the concentrations of $\mathrm{CO_2}$ in the gas phase and of the total dissolved inorganic carbon at the first step (eq. 56). According to Stumm and Morgan [29], $C_{DIC}$ at the first step has been fixed equal to $10^{-6}\mathrm{mol\,l^{-1}}$. This value has also been used to assess the initial concentration of $\mathrm{CO_2}$ in the gas phase, through eq. (58). The total alkalinity, $A_t$, at the first step has been

defined through eq. (71), as a function of the initial condition of $C_{DIC}$, $[H^+], [Ca^{2+}], [Na^+]$, $[K^+]$, $[Al^{3+}]$ and $[Mg^{2+}]$. Eqs. (65) and (66) highlight that the terms $\alpha_1$ and $\alpha_2$ are a function of $[H^+]$, thus of the initial soil pH which, as a generic value has been fixed equal to 7. The amount of adsorbed moles of $[H^+]$ on organic and clay colloids, $x_{H^+_{OM}}$ and $x_{H^+_{clay}}$, at the first step, has been calculated by solving an implicit system constituted by the algebraic equations related to the CEC component, thus by solving the system (A.1) excluding equations (4), (56), (58) and (71). Solving this algebraic implicit system resulted in the evaluation of $x_{Ca^{2+}_{OM}}$, $x_{Ca^{2+}_{clay}}$, $x_{Mg^{2+}_{OM}}$, $x_{Mg^{2+}_{clay}}$, $x_{Na^+_{OM}}$, $x_{Na^+_{clay}}$, $x_{K^+_{OM}}$, $x_{K^+_{clay}}$, $x_{Al^{3+}_{OM}}$ and $x_{Al^{3+}_{clay}}$ at the first step; therefore, the initial $Al_t{}^{3+}$, $Ca_t{}^{2+}$, $Mg_t{}^{2+}$, $K_t{}^+$ and $Na_t{}^+$ have been defined on the base of eqs. (70, 73-76). With reference to the initial total silicon in the system, a basic value of $10^{-11}$ mol $l^{-1}$ has been set.

A schematic representation of the numerical resolution of the model is provided in figure 3. At each time-step, after solving the soil water balance, forced with a stochastic rainfall, the output soil moisture, infiltration, leaching and evapotranspiration rates are coupled to the organic carbon balance, to obtain the decomposition rate and organic carbon concentration. For the sake of simplicity, the characteristics of vegetation are considered fixed in time; thus, the amount of litter added to the soil ($ADD$) is assumed as constant under a certain climate scenario (fixed values of $\alpha$ and $\lambda$). The output variables of these two balances are used to solve the explicit system. Once the initial conditions are fixed, the explicit system is firstly solved and its output variables, namely $C_t$, $A_t$, $Ca_t{}^{2+}$, $Na_t{}^+$, $Mg_t{}^{2+}$, $K_t^+$, $Al_t^{3+}$ and $Si_t$, can be passed to the implicit algebraic system (A.1). Once the implicit system

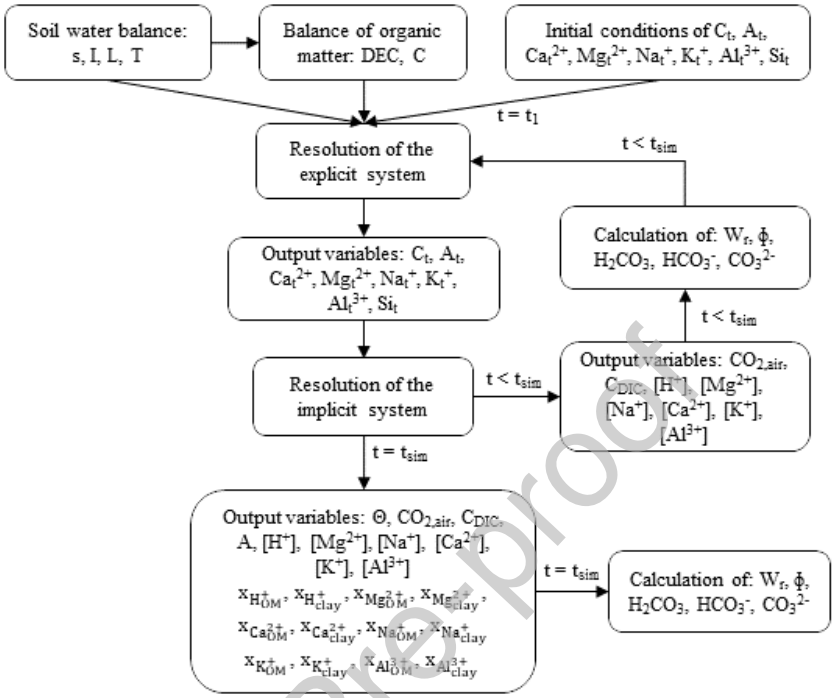


Figure 3: Schematic representation of the numerical resolution of the model. After solving the soil water and the organic matter balances, their output variables are passed to the explicit system. The simulation ends once the simulation end time is reached.

is solved, some of its output variables, such as the dissolved ions concentrations, can be used to solve the explicit system at the next time-step, since it is solved with a forward scheme. This goes on until the simulation end time is reached. It is worth recalling that the explicit system can be solved independently from the implicit one. Indeed, the resolution of the implicit part of the model can be carried out to obtain the time-series of individual variables (not combined), such as those of pH, $[Mg^{2+}]$, $[Na^+]$, $[K^+]$, $[Al^{3+}]$ and $[Ca^{2+}]$, that are very useful to see the effects of olivine on soil chemistry which could reflect on land management. The time-series of $[HCO_3^-]$ and

$[CO_3^{2-}]$ are very relevant as well, since they can be used to calculate the mass of carbon, translated into the equivalent mass of $CO_2$ on the base of the mass of carbon contained in a unit mass of $CO_2$, which is sequestered by olivine in a certain amount of time.

### *4.1. The role of wetness on weathering rate*

To shed light on the importance of soil moisture, plants and CEC, on weathering, we analyzed the time-series resulting from numerical solutions of the model. While here we consider more general characteristics, more specific applications will be presented in Cipolla et al. [1].

A first important result, shown in Figure 4, is that the relationship between olivine weathering rate and soil moisture is not single-valued. This is due to the nonlinearities in the relationship between soil moisture and soil biogeochemistry, i.e., the soil water balance and the implicit system of equations (A.1). The non-linear relationship between weathering rate and soil moisture (Fig. 4) reflects a typical hysteretic behavior. Figure 4a displays a time-series of soil moisture, and figure 4b the corresponding time-series of pH. Figure 4c shows the related olivine weathering rate, while the pattern of weathering rate with soil moisture with some grey arrows representative of the trajectories is plotted in figure 4d.

The hysteretic pattern of weathering rate with soil moisture highlights that the process maintains a memory of past events, such as the drying and wetting events. For a single soil moisture value there are two or more different weathering rate values, the lower ones related to the wetting period and the higher ones related to the drying one. This confirms that wetness is one of the most relevant factors controlling soil biogeochemistry and, in turn,

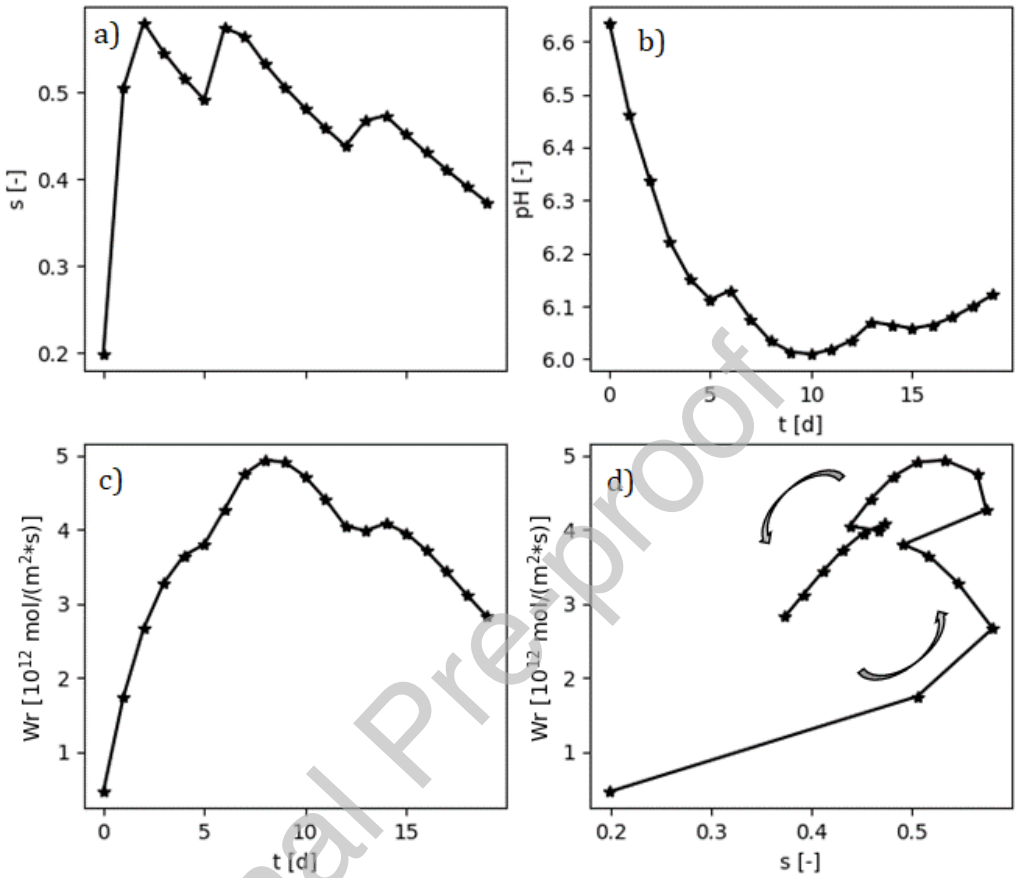


Figure 4: Time-series of soil moisture (a), pH (b), weathering rate (c) and pattern of weathering rate with soil moisture (d) with the grey arrows indicating the trajectories.

weathering rate [30, 31].

*4.2. The role of cation exchange processes on EW*

As it can be seen from the previous sections, the cation exchange plays an important role in the model. Depending on the equilibrium reactions regulating the exchanges between the dissolved ions in soil water and those adsorbed on soil colloids (29-30), significant variations in soil pH can be

expected, in turn impacting the olivine weathering rate. To understand the role of the cation exchange process on EW, it was instructive to look at the one-year time-series of soil water pH, of the sum of $Ca^{2+}$, $Mg^{2+}$, $Na^{+}$ and $K^{+}$ concentrations, indicated for brevity as nutrients, and of weathering rate for three different cation exchange capacity levels. The first one, indicated as 'No CEC', represents the condition in which CEC effects are negligible, the other one represents a typical cation exchange value (see, e.g., [8]), indicated as 'CEC', and the last one, named as 'Double CEC', represents an exceptionally high cation exchange capacity. In this last case, the CEC parameters values are the double of those presented in Weil and Brady [8], related to the 'CEC' scenario.

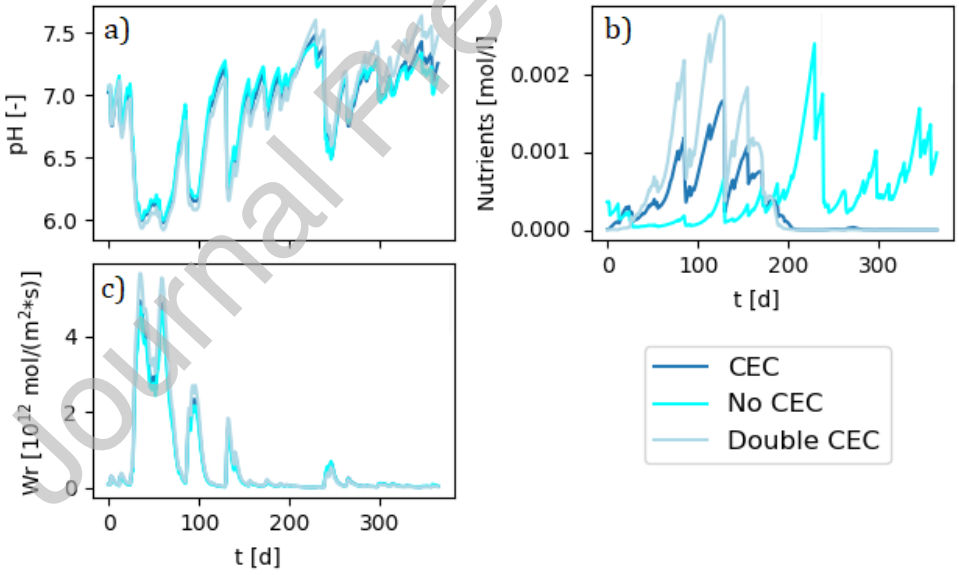


Figure 5: Time-series of soil water pH (a), of nutrients concentration in soil water (b) and of olivine weathering rate (c) under three different CEC levels.

As seen in figure 5b, in correspondence of the high values of the nutrients

concentration in soil water under the 'No CEC' level, approximately from day 200 to 365, there is a strong adsorption process as long as the cation exchange process is included, which becomes more relevant as the cation exchange capacity level increases. This happens because the cation exchanges are regulated by equilibrium reactions, thus if the concentration of dissolved ions is high, the adsorption process will be strong. On the other hand, in correspondence of the low values of the dissolved ions concentration under the 'No CEC' level, there is a weak adsorption of cations on soil colloids, resulting in a higher concentration in soil water. The same aspect can be found for the pH time-series (figure 5a). The pH variations due to different CEC levels reflect on weathering rate (figure 5c). Indeed, especially in correspondence of minimum pH values (e.g., approximately from day 30 to 90), a greater CEC results in a pH reduction, hence in a more accentuated peak of weathering rate.

All these aspects show the importance of a dynamical model which explicitly takes into account the cation exchange processes. The effects of these exchanges, regulated by equilibrium reactions, on soil biogeochemistry and, in turn, on EW dynamics become prominent over long time-scales, as they amplificate due to the nonlinearities.

### *4.3. The role of plants on soil biogeochemistry affecting EW*

Plants take up magnesium, calcium, potassium and sodium from soil water as common, important nutrients. In order to maintain a neutral balance, the excess of cation uptake is counteracted by a release of hydrogen ions in soil water, increasing soil water pH. To highlight the importance of this process in soil biogeochemical dynamics, a comparison of pH, weathering rate and

nutrients concentration time-series with and without plants uptake/release of ions is provided in figure 6.

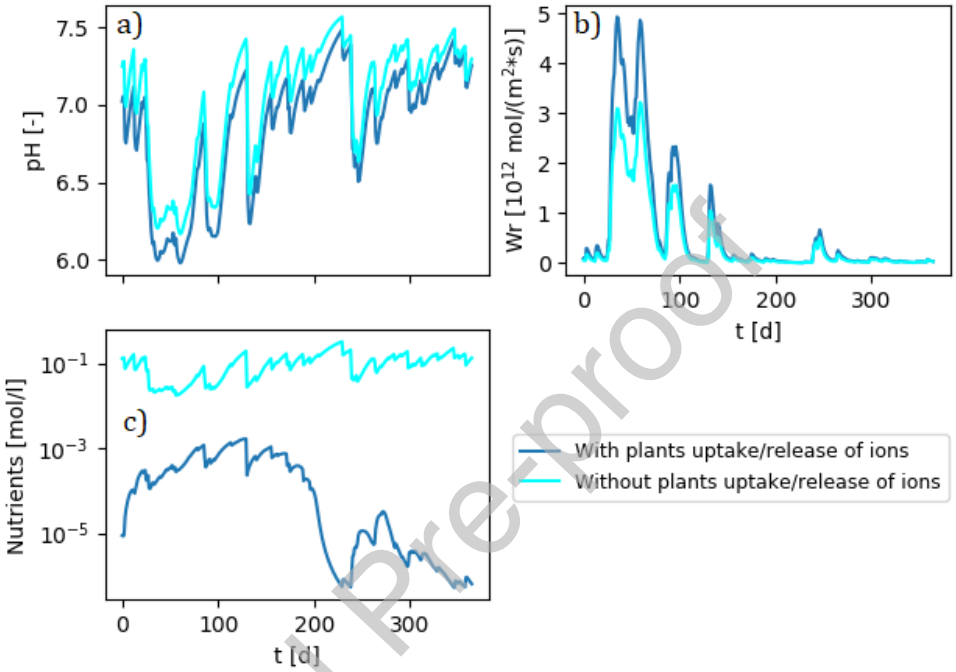


Figure 6: Time-series of soil pH (a), olivine weathering rate (b) and nutrients concentration in soil water (c) with and without the plants uptake/release of ions process.

Without plants uptake, the nutrients concentration in soil water is generally higher and less variable than in the case where the nutrients uptake is taken into account. In the latter case, the greater variability can be explained by the fact that the uptake is proportional to the transpiration rate, whose variability is inherited from rainfall. Consequently, without the release of hydrogen ions, soil pH is generally higher. This affects olivine weathering rate, since higher pH values correspond to lower weathering rates. These aspects clearly demonstrate the importance of correctly capturing the plants

uptake/release of ions when modeling EW applications.

## 5. Discussions

The inclusion of soil moisture, plant and soil organic matter-nutrient interactions in a biogeochemical-EW model provides a novel perspective on the key processes controlling the dissolution dynamics of olivine in field conditions. The resulting mathematical model, constituted by a system of eight differential equations and an implicit algebraic system consisting of twenty two equations, simultaneously considers stochasticity in soil moisture, time dynamics of organic matter decomposition and soil chemistry, soil cation exchange capacity, olivine dissolution and $CO_2$ consumption. To highlight the fundamental interactions between water, soil chemistry, and plants, EW was investigated in somewhat idealized conditions. Simplifying assumptions related to constant properties of rainfall, soil and vegetation can be easily relaxed. Detailed applications will be presented in Cipolla et al. [1].

The model can be extended in several directions. In this study, only the most common macro-nutrients for plants, namely $Mg^{2+}$, $K^+$ and the micro-nutrient $Na^+$, have been taken into account; however, the model can be expanded to include the nitrogen and phosphorous cycles (e.g., Porporato et al. [16], D'Odorico et al. [21]). In fact, a significant percentage of global natural land area is nitrogen and phosphorus limited [32] and the demand of nitrogen and phosphorus is generally considered to be high on a stoichiometric basis.

The carbon module of the model assumes a simple balance between an input of carbon from vegetation and a first-order decomposition term, with

constant carbon concentration in the biomass pool. More detailed carbon models can be analyzed and considered. For example, the recent non-linear "microbial models" may be used to couple microbial biomass, extracellular enzymes, and carbon substrate pools and take into account variations in the microbial carbon use efficiency in response to environmental conditions [33]. However, even if non-linear decomposition models may be more detailed over short time scales, simple linear parameterizations may be more suitable when considering long timescales [34].

One important source of uncertainty in EW is related to the estimation of weathering rates in the field. For instance, in the laboratory water quality and water/mineral contacts are well controlled, whereas in the field their characterization is rather difficult. Additionally, mineral weathering can be accelerated or slowed down by bacteria and fungi [35, 36], a process that remains largely unexplored in both lab and field settings. Here, we calibrated the rate constant based on Renforth et al. [7] in order to obtain a realistic order of magnitude for the weathering rates. However, further work in this direction is needed from both the experimental and modeling fronts to improve estimates of field reaction rates.

Another source of uncertainty that affects the estimation of field weathering rate is connected to the distribution of olivine particles diameter, resulting from the grinding operation. In our model, we considered a single effective diameter, mainly for the sake of simplicity. In fact, tracking the actual evolution of particle size distributions would considerably increase the complexity and computational cost of the model. As an illustration, we show in Figure 7 how different particle diameters affect olivine weathering

rate, considering three particle sizes based on the particle size distribution of Renforth et al. [7].

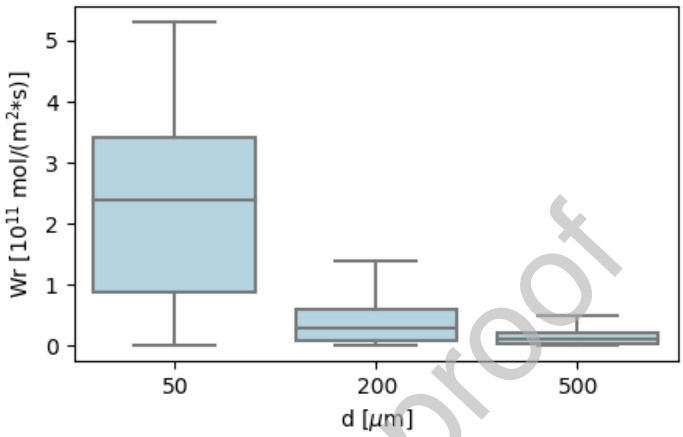


Figure 7: Box plot related to the olivine weathering rate computed at three different particle sizes.

As the particle size decreases, the weathering rate tends to increase at a quadratic rate, due to its quadratic relationship with the specific surface area (see eq. 28). While it is tempting to use small particle sizes, one should bear in mind that reducing particle size leads to higher grinding costs and $CO_2$ emissions (i.e., greater amount of energy needed to grind particles to a smaller size). In view of practical EW applications, a balance between these factors is fundamental to ensure that the carbon sink of EW more than compensates for the $CO_2$ emissions and that the intervention is cost-effective.

It would also be important to analyze the role of temporal (e.g., seasonal and interannual) variability of the rainfall forcing and vegetation dynamics, e.g. litter and potential transpiration rate. In agroecosystems, for example, crop growth and harvest should be taken into account, including how

they affect nutrient cycling. Other land management practices (e.g., organic amendment via manure or compost) should also be analyzed in terms of its synergies with EW.

Several components considered here could be included in reactive transport models. For example, the APSIM model [37] simulates, at a site scale, crop growth, soil organic matter, pH time dynamics and soil water balance. However, it does not consider the cation exchange capacity and all the weathering processes of the naturally present minerals in soil. The Sheffield model [20] instead is able to simulate, at a global scale, the $CO_2$ consumption for EW and the soil chemistry dynamics, also taking into account the effects of EW on ocean acidification. However, due to the spatial scale of interest it does not consider crop growth and cation exchange processes. Our model considers the cation exchange processes, which are very important in the evaluation of the dissolved ions concentrations in soil water, and is also able to calculate the net sink of $CO_2$ from a certain mass of added olivine at a site scale. It considers unpredictable variability in soil moisture in the form of a stochastic process; this is fundamental to understand the role of hydrological variability on EW. As our results showed, the interaction between these processes largely controls the trajectory of olivine dissolution over time and, if not accounted for, uncertainties and errors may amplify over time due to nonlinearities in the relationship between hydrology, soil biogeochemistry, and plants.

## 6. Conclusions

This paper presents a model that couples biogeochemical and ecohydrological processes involved in the weathering process of olivine. Placing special attention to field conditions, the main scope of the model is to simulate the dynamics of olivine weathering rate within a vegetated soil and to understand $CO_2$ sequestration potential of EW. The model is structured in different interconnected components and the resulting scheme consists of an explicit system of eight mass balance total differential equations and an implicit part with twenty two algebraic equations in twenty two unknown variables. The model stresses the pivotal role of hydrology on the soil biogeochemistry, plants dynamics and, in turn, the olivine weathering rate. We also paid particular attention to the time dynamics of soil water pH, both with and without olivine, since this is an important parameter for many aspects, such as the dissolved ions concentration dynamics and the suitability of the environment for plants.

The results highlight how the dependence between weathering rate and soil moisture is characterized by a hysteretic behavior, due to nonlinearities and memory effects, and that cation exchange and plants uptake/release of ions processes, which are not always included in the existing reactive transport models, exert a strong control on olivine weathering rates. Cipolla et al. [1] describes a first application of the proposed model to evaluate olivine dissolution dynamics and its effects on carbon sequestration under different climate scenarios and land carbon managements (e.g., organic amendment).

## Appendix A. Implicit algebraic system derivation

The implicit system (A.1) consists of 22 equations in 22 unknown terms, namely $\Theta$, $CO_{2,\mathrm{air}}$, $C_{DIC}$, $A$, $[H^+]$, $[Mg^{2+}]$, $[Na^+]$, $[K^+]$, $[Al^{3+}]$, $[Ca^{2+}]$, $x_{H^+_{OM}}$, $x_{H^+_{clay}}$, $x_{Mg^{2+}_{OM}}$, $x_{Mg^{2+}_{clay}}$, $x_{Ca^{2+}_{OM}}$, $x_{Ca^{2+}_{clay}}$, $x_{Na^+_{OM}}$, $x_{Na^+_{clay}}$, $x_{K^+_{OM}}$, $x_{K^+_{clay}}$, $x_{Al^{3+}_{OM}}$, $x_{Al^{3+}_{clay}}$. It has been derivated by putting together many of the model equations and, for the sake of a better readability, is presented as,

$$
\begin{cases}
\Theta = \frac{[\mathrm{Mg^{2+}}]^{\frac{1}{2}}[\mathrm{H_2SiO_3}]^{\frac{1}{4}}}{[\mathrm{H^+}]} \\
C_t = [\mathrm{CO_{2,air}}] + C_{DIC} \\
K_{H,ad} = \frac{[\mathrm{H_2CO_3}^*]}{[\mathrm{CO_{2,air}}]} \\
A_t = C_{DIC}(\alpha_1 + 2\alpha_2) - [\mathrm{H_t}^+] + [\mathrm{OH^-}] - 3[\mathrm{Al}_t^{3+}] \\
\mathrm{H_t}^+ = \mathrm{H}^+ + x_{\mathrm{H^+_{OM}}} + x_{\mathrm{H^+_{clay}}} \\
\mathrm{Ca_t}^{2+} = \mathrm{Ca}^{2+} + x_{\mathrm{Ca^{2+}_{OM}}} + x_{\mathrm{Ca^{2+}_{clay}}} \\
\mathrm{Mg_t}^{2+} = \mathrm{Mg}^{2+} + x_{\mathrm{Mg^{2+}_{OM}}} + x_{\mathrm{Mg^{2+}_{clay}}} \\
\mathrm{Na_t}^{+} = \mathrm{Na}^{+} + x_{\mathrm{Na^{+}_{OM}}} + x_{\mathrm{Na^{+}_{clay}}} \\
\mathrm{K}_t^{+} = \mathrm{K}^{+} + x_{\mathrm{K}^+_{OM}} + x_{\mathrm{K}^+_{clay}} \\
\mathrm{Al}_t^{3+} = \mathrm{Al}^{3+} + x_{\mathrm{Al}^{3+}_{OM}} + x_{\mathrm{Al}^{3+}_{clay}} \\
x_{\mathrm{H^+_{OM}}} = \frac{CEC_{OM} - x_{\mathrm{Na^+_{OM}}} - x_{\mathrm{Mg^{2+}_{OM}}} - x_{\mathrm{K}^+_{OM}} - x_{\mathrm{Al}^{3+}_{OM}}}{[1 + \frac{1}{SC_{OM}(\mathrm{H^+ - Ca^{2+}})\frac{[\mathrm{H^+}]}{[\mathrm{Ca^{2+}}]^{\frac{1}{2}}}}]} \\
x_{\mathrm{H^+_{clay}}} = \frac{CEC_{clay} - x_{\mathrm{Na^+_{clay}}} - x_{\mathrm{Mg^{2+}_{clay}}} - x_{\mathrm{K}^+_{clay}} - x_{\mathrm{Al}^{3+}_{clay}}}{[1 + \frac{1}{SC_{clay}(\mathrm{H^+ - Ca^{2+}})\frac{[\mathrm{H^+}]}{[\mathrm{Ca^{2+}}]^{\frac{1}{2}}}}]} \\
x_{\mathrm{Mg^{2+}_{OM}}} = \frac{CEC_{OM} - x_{\mathrm{Na^+_{OM}}} - x_{\mathrm{H^+_{OM}}} - x_{\mathrm{K}^+_{OM}} - x_{\mathrm{Al}^{3+}_{OM}}}{[1 + \frac{1}{SC_{OM}(\mathrm{Ca^{2+} - Mg^{2+}})\frac{[\mathrm{Mg^{2+}}]}{[\mathrm{Ca^{2+}}]}}]} \\
x_{\mathrm{Mg^{2+}_{clay}}} = \frac{CEC_{clay} - x_{\mathrm{Na^+_{clay}}} - x_{\mathrm{H^+_{clay}}} - x_{\mathrm{K}^+_{clay}} - x_{\mathrm{Al}^{3+}_{clay}}}{[1 + \frac{1}{SC_{clay}(\mathrm{Ca^{2+} - Mg^{2+}})\frac{[\mathrm{Mg^{2+}}]}{[\mathrm{Ca^{2+}}]}}]} \\
x_{\mathrm{Na^+_{OM}}} = \frac{CEC_{OM} - x_{\mathrm{H^+_{OM}}} - x_{\mathrm{Mg^{2+}_{OM}}} - x_{\mathrm{K}^+_{OM}} - x_{\mathrm{Al}^{3+}_{OM}}}{[1 + \frac{1}{SC_{OM}(\mathrm{Na^+ - Ca^{2+}})\frac{[\mathrm{Na^+}]}{[\mathrm{Ca^{2+}}]^{\frac{1}{2}}}}]} \\
x_{\mathrm{Na^+_{clay}}} = \frac{CEC_{clay} - x_{\mathrm{H^+_{clay}}} - x_{\mathrm{Mg^{2+}_{clay}}} - x_{\mathrm{K}^+_{clay}} - x_{\mathrm{Al}^{3+}_{clay}}}{[1 + \frac{1}{SC_{clay}(\mathrm{Na^+ - Ca^{2+}})\frac{[\mathrm{Na^+}]}{[\mathrm{Ca^{2+}}]^{\frac{1}{2}}}}]} \\
x_{\mathrm{K}^+_{OM}} = \frac{CEC_{OM} - x_{\mathrm{H^+_{OM}}} - x_{\mathrm{Mg^{2+}_{OM}}} - x_{\mathrm{Na^+_{OM}}} - x_{\mathrm{Al}^{3+}_{OM}}}{[1 + \frac{1}{SC_{OM}(\mathrm{K^+ - Ca^{2+}})\frac{[\mathrm{K^+}]}{[\mathrm{Ca^{2+}}]^{\frac{1}{2}}}}]} \\
x_{\mathrm{K}^+_{clay}} = \frac{CEC_{clay} - x_{\mathrm{H^+_{clay}}} - x_{\mathrm{Mg^{2+}_{clay}}} - x_{\mathrm{Na^+_{clay}}} - x_{\mathrm{Al}^{3+}_{clay}}}{[1 + \frac{1}{SC_{clay}(\mathrm{K^+ - Ca^{2+}})\frac{[\mathrm{K^+}]}{[\mathrm{Ca^{2+}}]^{\frac{1}{2}}}}]} \\
x_{\mathrm{Al^{3+}_{OM}}} = \frac{CEC_{OM} - x_{\mathrm{H^+_{OM}}} - x_{\mathrm{Mg^{2+}_{OM}}} - x_{\mathrm{Na^+_{OM}}} - x_{\mathrm{K}^+_{OM}}}{[1 + \frac{1}{SC_{OM}(\mathrm{Al^{3+} - Ca^{2+}})\frac{[\mathrm{Al^{3+}}]^{\frac{1}{3}}}{[\mathrm{Ca^{2+}}]^{\frac{1}{2}}}}]} \\
x_{\mathrm{Al^{3+}_{clay}}} = \frac{CEC_{clay} - x_{\mathrm{H^+_{clay}}} - x_{\mathrm{Mg^{2+}_{clay}}} - x_{\mathrm{Na^+_{clay}}} - x_{\mathrm{K}^+_{clay}}}{[1 + \frac{1}{SC_{clay}(\mathrm{Al^{3+} - Ca^{2+}})\frac{[\mathrm{Al^{3+}}]^{\frac{1}{3}}}{[\mathrm{Ca^{2+}}]^{\frac{1}{2}}}}]} \\
CEC_{OM} = x_{\mathrm{H^+_{OM}}} + x_{\mathrm{Na^+_{OM}}} + x_{\mathrm{Ca^{2+}_{OM}}} + x_{\mathrm{Mg^{2+}_{OM}}} + x_{\mathrm{K}^+_{OM}} + x_{\mathrm{Al}^{3+}_{OM}} \\
CEC_{clay} = x_{\mathrm{H^+_{clay}}} + x_{\mathrm{Na^+_{clay}}} + x_{\mathrm{Ca^{2+}_{clay}}} + x_{\mathrm{Mg^{2+}_{clay}}} + x_{\mathrm{K}^+_{clay}} + x_{\mathrm{Al}^{3+}_{clay}}
\end{cases}
\tag{A.1}
$$

## Appendix B. List of abbreviations

| | | |
|---|---|---|
| $s$ | Soil moisture | |
| $s_{fc}$ | Soil moisture at field capacity | |
| $W_r$ | Weathering rate | mol $m^{-2}s^{-1}$ |
| pH | Soil pH | |
| $k_{sil}$ | Dissolution rate constant of forsterite | mol $m^{-2}s^{-1}$ |
| $\Theta$ | Ion activity product | |
| $k_{eq}$ | Olivine dissolution constant | |
| $\phi$ | Effective diameter of olivine particles | $\mu$m |
| $V_M$ | Molar volume of olivine | $cm^3mol^{-1}$ |
| C | Organic carbon concentration | gC $m^{-3}$ |
| $ADD$ | Average added litter | gC $m^{-2}d^{-1}$ |
| $r$ | Fraction of decomposed carbon to respiration | |
| $DEC$ | Decomposed organic carbon | gC $m^{-2}d^{-1}$ |
| $k_{DEC}$ | Carbon decomposition constant | $m^3d^{-1}gC^{-1}$ |
| $C_b$ | Carbon concentration in the biomass pool | gC $m^{-3}$ |
| $D$ | $CO_2$ diffusivity in the soil | $m^2s^{-1}$ |
| $D_0$ | Free-air diffusion coefficient of $CO_2$ | $m^2s^{-1}$ |
| $Z_r$ | Soil depth | m |
| $n$ | Soil porosity | |
| $CO_{2,atm}$ | Atmospheric $CO_2$ concentration | ppm |
| $k_1$ | First dissociation constant of carbonic acid | |
| $k_2$ | Second dissociation constant of carbonic acid | |
| $k_w$ | Self-ionization constant of water | |
| $PI$ | Input of $H^+$ from plants | $mol_{H^+}l^{-1}$ |
| $RI$ | Input of $H^+$ from rainfall | $mol_{H^+}l^{-1}$ |
| $W_{bg}$ | Background weathering term | $mol_{H^+}$ |
| $W_{oliv}$ | Olivine weathering term | $mol_{H^+}$ |
| $x_{M^{m+}_{OM}}$ | Mass of adsorbed of a generic ion on organic colloids | $mol_{M^{m+}}$ |
| $x_{M^{m+}_{clay}}$ | Mass of adsorbed of a generic ion on clay colloids | $mol_{M^{m+}}$ |

| | | |
|---|---|---|
| $UP_{\mathrm{M}}$ | Plant uptake of a generic ion | $\mathrm{mol_M l^{-1}}$ |
| $k_{bg}$ | Specific dissolution rate of background minerals | $\mathrm{mol\ m^{-2} s^{-1}}$ |
| $d_{bg}$ | Diameter of background minerals particles | $\mu$m |
| $f_{bg}$ | Mass fraction of background minerals | |
| $\rho_b$ | Soil bulk density | $\mathrm{kg\ m^{-3}}$ |
| $\rho_{bg}$ | Density of background minerals | $\mathrm{g\ cm^{-3}}$ |
| $V_{bg}$ | Volume of a particle of background minerals | $\mathrm{cm^3}$ |
| $M_{oliv}$ | Mass of added olivine | $\mathrm{g\ m^{-2}}$ |
| $\rho_{oliv}$ | Density of olivine | $\mathrm{g\ cm^{-3}}$ |
| $V_{oliv}$ | Volume of a particle of olivine | $\mathrm{cm^3}$ |
| $CEC_{OM}$ | Organic component of the soil cation exchange capacity | mol |
| $CEC_{clay}$ | Clay component of the soil cation exchange capacity | mol |
| $SC_{OM}(\mathrm{X-M})$ | Selectivity constant for a generic exchange on organic colloids | |
| $SC_{clay}(\mathrm{X-M})$ | Selectivity constant for a generic exchange on clay colloids | |
| $C_{DIC}$ | Total dissolved inorganic carbon | $\mathrm{mol\ l^{-1}}$ |
| $C_t$ | Total carbon | $\mathrm{mol\ l^{-1}}$ |
| $K_{H,ad}$ | Adimensional Henry's constant | |
| $A$ | Alkalinity | $\mathrm{mol\ l^{-1}}$ |
| $A_t$ | Total alkalinity | $\mathrm{mol\ l^{-1}}$ |
| $\mathrm{H_t^+}$ | Moles of total $\mathrm{H^+}$ | mol |
| $\mathrm{Ca_t^{2+}}$ | Moles of total $\mathrm{Ca^{2+}}$ | mol |
| $\mathrm{Mg_t^{2+}}$ | Moles of total $\mathrm{Mg^{2+}}$ | mol |
| $\mathrm{Na_t^+}$ | Moles of total $\mathrm{Na^+}$ | mol |
| $\mathrm{K_t^+}$ | Moles of total $\mathrm{K^+}$ | mol |
| $\mathrm{Al_t^{3+}}$ | Moles of total $\mathrm{Al^{3+}}$ | mol |

## References

[1] G. Cipolla, S. Calabrese, L. V. Noto, A. Porporato, The role of hydrology on enhanced weathering for carbon sequestration. ii. exploring solutions to increase olivine

weathering rate and carbon sequestration in field, Submitted to: Advances in Water Resources (2020).

[2] A. Arneth, F. Denton, F. Agus, A. Elbehri, K. Erb, B. Osman Elasha, M. Rahimi, M. Rounsevell, A. Spence, R. Valentini, Framing and context. in: Climate change and land: an ipcc special report on climate change, desertification, land degradation, sustainable land management, food security, and greenhouse gas fluxes in terrestrial ecosystems, 2019.

[3] T. M. Lenton, Early warning of climate tipping points, Nature Climate Change 1 (2011). URL: https://doi.org/10.1038/nclimate1143. doi:10.1038/nclimate1143.

[4] J. Hartmann, A. J. West, P. Renforth, P. Köhler, C. L. De La Rocha, D. A. Wolf-Gladrow, H. H. Dürr, J. Scheffran, Enhanced chemical weathering as a geoengineering strategy to reduce atmospheric carbon dioxide, supply nutrients, and mitigate ocean acidification, Reviews of Geophysics 51 (2013) 113–149. URL: https://agupubs.onlinelibrary.wiley.com/doi/abs/10.1002/rog.20004. doi:10.1002/rog.20004.

[5] L. L. Taylor, D. J. Beerling, S. Quegan, S. A. Banwart, Simulating carbon capture by enhanced weathering with croplands: an overview of key processes highlighting areas of future model development, Biology Letters 13 (2017) 20160868. URL: https://royalsocietypublishing.org/doi/abs/10.1098/rsbl.2016.0868. doi:10.1098/rsbl.2016.0868.

[6] H. F. M. ten Berge, H. G. van der Meer, J. W. Steenhuizen, P. W. Goedhart, P. Knops, J. Verhagen, Olivine weathering in soil, and its effects on growth and nutrient uptake in ryegrass (lolium perenne l.): A pot experiment, PLOS ONE 7 (2012) 1–8. URL: https://doi.org/10.1371/journal.pone.0042098. doi:10.1371/journal.pone.0042098.

[7] P. Renforth, P. P. von Strandmann], G. Henderson, The dissolution of olivine added to soil: Implications for enhanced weathering, Applied Geochemistry 61 (2015) 109

– 118. URL: http://www.sciencedirect.com/science/article/pii/S0883292715001389. doi:https://doi.org/10.1016/j.apgeochem.2015.05.016.

[8] R. Weil, N. Brady, The Nature and Properties of Soils. 15th edition, 2017.

[9] H. Sverdrup, P. Warfvinge, Weathering of primary silicate minerals in the natural soil environment in relation to a chemical weathering model, Water, Air, and Soil Pollution 38 (1988) 387–408. URL: https://doi.org/10.1007/BF00280768. doi:10.1007/bf00280768.

[10] A. C. Lasaga, Chemical kinetics of water-rock interactions, Journal of Geophysical Research: Solid Earth 89 (1984) 4009–4025. URL: https://agupubs.onlinelibrary.wiley.com/doi/abs/10.1029/JB089iB06p04009. doi:10.1029/JB089iB06p04009.

[11] P. Köhler, J. Hartmann, D. A. Wolf-Gladrow, Geoengineering potential of artificially enhanced silicate weathering of olivine, Proceedings of the National Academy of Sciences 107 (2010) 20228–20233. URL: https://www.pnas.org/content/107/47/20228. doi:10.1073/pnas.1000545107.

[12] J. L. Palandri, Y. K. Kharaka, A compilation of rate parameters of water-mineral interaction kinetics for application to geochemical modeling, U.S. Geological Survey Open File Report 2004-1068, 2004, p. 64.

[13] J. D. Rimstidt, Diffusion control of quartz and forsterite dissolution rates, Applied Geochemistry 61 (2015) 99 – 108. URL: http://www.sciencedirect.com/science/article/pii/S0883292715001420. doi:https://doi.org/10.1016/j.apgeochem.2015.05.020.

[14] A. F. White, S. L. Brantley, The effect of time on the weathering of silicate minerals: why do weathering rates differ in the laboratory and field?, Chemical Geology 202 (2003) 479 – 506. URL: http://www.sciencedirect.com/science/article/pii/

S0009254103002560. doi:https://doi.org/10.1016/
j.chemgeo.2003.03.001, controls on Chemical Weathering.

[15] A. McCauley, C. Jones, K. Olson-Rutz, Soil ph and organic matter, in: Nutrient Management Module No. 8, Montana State University Extension Service, Bozeman, Montana, 2017, pp. 1–12.

[16] A. Porporato, P. D'Odorico, F. Laio, I. Rodriguez-Iturbe, Hydrologic controls on soil carbon and nitrogen cycles. i. modeling scheme, Advances in Water Resources 26 (2003) 45–58. URL: http://www.sciencedirect.com/science/article/pii/S0309170802000945. doi:https://doi.org/10.1016/S0309-1708(02)00094-5.

[17] F. Morel, J. Hering, Principles and Applications of Aquatic Chemistry, 1993.

[18] K. Maher, C. I. Steefel, A. F. White, D. A. Stonestrom, The role of reaction affinity and secondary minerals in regulating chemical weathering rates at the santa cruz soil chronosequence, california, Geochimica et Cosmochimica Acta 73 (2009) 2804 – 2831. URL: http://www.sciencedirect.com/science/article/pii/S0016703709000775. doi:https://doi.org/10.1016/j.gca.2009.01.030.

[19] K. Maher, The dependence of chemical weathering rates on fluid residence time, Earth and Planetary Science Letters 294 (2010) 101 – 110. URL: http://www.sciencedirect.com/science/article/pii/S0012821X10001810. doi:https://doi.org/10.1016/j.epsl.2010.03.010.

[20] L. L. Taylor, J. Quirk, R. M. S. Thorley, P. A. Kharecha, J. Hansen, A. Ridgwell, M. R. Lomas, S. A. Banwart, D. J. Beerling, Enhanced weathering strategies for stabilizing climate and averting ocean acidification, Nature Climate Change 6 (2016) 402–406. URL: https://doi.org/10.1038/nclimate2882. doi:10.1038/nclimate2882.

[21] P. D'Odorico, F. Laio, A. Porporato, I. Rodriguez-Iturbe, Hydrologic controls on soil carbon and nitrogen cycles. ii. a case study, Advances in Water Resources 26 (2003)

59 – 70. URL: http://www.sciencedirect.com/science/article/pii/S0309170802000957. doi:https://doi.org/10.1016/S0309-1708(02)00095-7.

[22] E. Daly, A. C. Oishi, A. Porporato, G. G. Katul, A stochastic model for daily subsurface co2 concentration and related soil respiration, Advances in Water Resources 31 (2008) 987 – 994. URL: http://www.sciencedirect.com/science/article/pii/S0309170808000559. doi:https://doi.org/10.1016/j.advwatres.2008.04.001.

[23] W. J. Riley, Z. M. Subin, D. M. Lawrence, S. C. Swenson, M. S. Torn, L. Meng, N. M. Mahowald, P. Hess, Barriers to predicting changes in global terrestrial methane fluxes: analyses using clm4me, a methane biogeochemistry model integrated in cesm, Biogeosciences 8 (2011) 1925–1953. URL: https://www.biogeosciences.net/8/1925/2011/. doi:10.5194/bg-8-1925-2011.

[24] K. Rice, F. J. Deviney, G. Olson, Acid rain in shenandoah national park, virginia, U.S. Geological Survey Fact Sheet 2007–3057, 2007, p. 4.

[25] N. Coleman, A. Mehlich, The chemistry of soil ph, USDA Yearbook, Washington, DC, USA, 1957, pp. 72–79.

[26] D. L. Suarez, J. Simunek, Unsatchem: Unsaturated water and solute transport model with equilibrium and kinetic chemistry, Soil Science Society of America Journal 61 (1997) 1633–1646. URL: https://acsess.onlinelibrary.wiley.com/doi/abs/10.2136/sssaj1997.03615995006100060014x. doi:10.2136/sssaj1997.03615995006100060014x.

[27] Y. Mau, A. Porporato, A dynamical system approach to soil salinity and sodicity, Advances in Water Resources 83 (2015) 68 – 76. URL: http://www.sciencedirect.com/science/article/pii/S0309170815001037. doi:https://doi.org/10.1016/j.advwatres.2015.05.010.

[28] I. Rodriguez-Iturbe, A. Porporato, L. Ridolfi, V. Isham, D. R. Coxi, Probabilistic modelling of water balance at a point: the role of climate, soil and vegetation, Proceedings of the Royal Society of London. Series A: Mathematical, Physical and Engineering Sciences 455 (1999) 3789–3805. URL: https://royalsocietypublishing.org/doi/abs/10.1098/rspa.1999.0477. doi:10.1098/rspa.1999.0477.

[29] W. Stumm, J. Morgan, Aquatic Chemistry: Chemical Equilibria and Rates in Natural Waters, 1995.

[30] S. Calabrese, A. J. Parolari, A. Porporato, Hydrologic transport of dissolved inorganic carbon and its control on chemical weathering, Journal of Geophysical Research: Earth Surface 122 (2017) 2016–2032. URL: https://agupubs.onlinelibrary.wiley.com/doi/abs/10.1002/2017JF004346. doi:10.1002/2017JF004346.

[31] S. Calabrese, A. Porporato, Wetness controls on global chemical weathering, Environmental Research Communications 2 (2020) 085005. doi:10.1088/2515-7620/abad7b.

[32] E. Du, C. Terrer, A. F. A. Pellegrini, A. Ahlström, C. J. van Lissa, X. Zhao, N. Xia, X. Wu, R. B. Jackson, Global patterns of terrestrial nitrogen and phosphorus limitation, Nature Geoscience 13 (2020) 221–226. URL: https://doi.org/10.1038/s41561-019-0530-4. doi:10.1038/s41561-019-0530-4.

[33] W. R. Wieder, S. D. Allison, E. A. Davidson, K. Georgiou, O. Hararuk, Y. He, F. Hopkins, Y. Luo, M. J. Smith, B. Sulman, K. Todd-Brown, Y.-P. Wang, J. Xia, X. Xu, Explicitly representing soil microbial processes in earth system models, Global Biogeochemical Cycles 29 (2015) 1782–1800. URL: https://agupubs.onlinelibrary.wiley.com/doi/abs/10.1002/2015GB005188. doi:10.1002/2015GB005188. arXiv:https://agupubs.onlinelibrary.wiley.com/doi/pdf/10.1002/2015GB005188.

[34] S. Manzoni, A. Porporato, Soil carbon and nitrogen mineralization: theory and models across scales, Soil Biology and Biochemistry 41 (2009) 1355–1379.

[35] S. Uroz, C. Calvaruso, M.-P. Turpault, P. Frey-Klett, Mineral weathering by bacteria: ecology, actors and mechanisms, Trends in Microbiology 17 (2009) 378 – 387. URL: http://www.sciencedirect.com/science/article/pii/S0966842X09001279. doi:https://doi.org/10.1016/j.tim.2009.05.004.

[36] S. Bonneville, M. M. Smits, A. Brown, J. Harrington, J. R. Leake, R. Brydson, L. G. Benning, Plant-driven fungal weathering: Early stages of mineral alteration at the nanometer scale, Geology 37 (2009) 615–618. URL: https://doi.org/10.1130/G25699A.1. doi:10.1130/G25699A.1. arXiv:https://pubs.geoscienceworld.org/geology/article-pdf/37/7/615/3536763/i0091-7613-37-7-615.pdf.

[37] B. Keating, P. Carberry, G. Hammer, M. Probert, M. Robertson, D. Holzworth, N. Huth, J. Hargreaves, H. Meinke, Z. Hochman, G. McLean, K. Verburg, V. Snow, J. Dimes, M. Silburn, E. Wang, S. Brown, K. Bristow, S. Asseng, S. Chapman, R. McCown, D. Freebairn, C. Smith, An overview of apsim, a model designed for farming systems simulation, European Journal of Agronomy 18 (2003) 267 – 288. URL: http://www.sciencedirect.com/science/article/pii/S1161030102001089. doi:https://doi.org/10.1016/S1161-0301(02)00108-9, modelling Cropping Systems: Science, Software and Applications.

**Declaration of interests**

☒ The authors declare that they have no known competing financial interests or personal relationships that could have appeared to influence the work reported in this paper.

☐The authors declare the following financial interests/personal relationships which may be considered as potential competing interests:

**Giuseppe Cipolla:** Conceptualization, Methodology, Software, Formal analysis, Investigation, Data Curation, Writing - Original Draft, Visualization;

**Salvatore Calabrese**: Conceptualization, Methodology, Validation, Writing - Review & Editing, Visualization, Supervision, Project administration;

**Leonardo Valerio Noto**: Conceptualization, Validation, Resources, Writing - Review & Editing, Supervision, Project administration;

**Amilcare Porporato**: Conceptualization, Validation, Resources, Writing - Review & Editing, Supervision, Project administration, Funding acquisition.